



**NAVAL
POSTGRADUATE
SCHOOL**

MONTEREY, CALIFORNIA

THESIS

**SCARF JOINT MODELING AND ANALYSIS OF
COMPOSITE MATERIALS**

by

Armando Marrón

June 2009

Thesis Advisor:
Second Reader:

Young W. Kwon
Douglas C. Loup

Approved for public release; distribution is unlimited.

THIS PAGE INTENTIONALLY LEFT BLANK

REPORT DOCUMENTATION PAGE			Form Approved OMB No. 0704-0188	
Public reporting burden for this collection of information is estimated to average 1 hour per response, including the time for reviewing instruction, searching existing data sources, gathering and maintaining the data needed, and completing and reviewing the collection of information. Send comments regarding this burden estimate or any other aspect of this collection of information, including suggestions for reducing this burden, to Washington headquarters Services, Directorate for Information Operations and Reports, 1215 Jefferson Davis Highway, Suite 1204, Arlington, VA 22202-4302, and to the Office of Management and Budget, Paperwork Reduction Project (0704-0188) Washington DC 20503.				
1. AGENCY USE ONLY (Leave blank)		2. REPORT DATE June 2009	3. REPORT TYPE AND DATES COVERED Master's Thesis	
4. TITLE AND SUBTITLE Scarf Joint Modeling and Analysis of Composite Materials			5. FUNDING NUMBERS	
6. AUTHOR(S) Armando Marron			8. PERFORMING ORGANIZATION REPORT NUMBER	
7. PERFORMING ORGANIZATION NAME(S) AND ADDRESS(ES) Naval Postgraduate School Monterey, CA 93943-5000			10. SPONSORING/MONITORING AGENCY REPORT NUMBER	
9. SPONSORING /MONITORING AGENCY NAME(S) AND ADDRESS(ES) N/A			11. SUPPLEMENTARY NOTES The views expressed in this thesis are those of the author and do not reflect the official policy or position of the Department of Defense or the U.S. Government.	
12a. DISTRIBUTION / AVAILABILITY STATEMENT Approved for public release; distribution is unlimited.			12b. DISTRIBUTION CODE	
13. ABSTRACT (maximum 200 words) The objective of this study is to investigate joint strength of the scarf joint configuration, constructed from carbon and glass woven fabric hybrid laminates, with different material combinations. Glass/glass, glass/carbon, carbon/glass, and carbon/carbon are tested under various loading conditions like tension, compression, bending and shear loading. Both experimental and computational studies are conducted. For the experimental study, specimens made of scarf joints using carbon and glass woven fabrics are tested under compressive loadings to determine their joint failure strengths. Computational models are then developed to predict the joint strengths under the same conditions as in the experiments using the discrete resin layer model along with fracture mechanics and virtual crack closure techniques. The comparisons are good. Once the computational models are validated from the test results, the scarf joint strengths are computed under different loading conditions.				
14. SUBJECT TERMS scarf joint, finite element method, energy release rate, virtual crack closure method, ansys, composites, overlap joint, fracture mechanics			15. NUMBER OF PAGES 77	
			16. PRICE CODE	
17. SECURITY CLASSIFICATION OF REPORT Unclassified	18. SECURITY CLASSIFICATION OF THIS PAGE Unclassified	19. SECURITY CLASSIFICATION OF ABSTRACT Unclassified	20. LIMITATION OF ABSTRACT UU	

THIS PAGE INTENTIONALLY LEFT BLANK

Approved for public release; distribution is unlimited

SCARF JOINT MODELING AND ANALYSIS OF COMPOSITE MATERIALS

Armando Marrón
Lieutenant, United States Navy
B.S., California Polytechnic State University, SLO, 2001

Submitted in partial fulfillment of the
requirements for the degree of

MASTER OF SCIENCE IN MECHANICAL ENGINEERING

from the

**NAVAL POSTGRADUATE SCHOOL
June 2009**

Author: Armando Marrón

Approved by: Professor Young W. Kwon
Thesis Advisor

Douglas C. Loup
Second Reader

Knox T. Millsaps
Chairman, Department of Mechanical and
Astronautical Engineering

THIS PAGE INTENTIONALLY LEFT BLANK

ABSTRACT

The objective of this study is to investigate joint strength of the scarf joint configuration, constructed from carbon and glass woven fabric hybrid laminates, with different material combinations. Glass/glass, glass/carbon, carbon/glass, and carbon/carbon are tested under various loading conditions like tension, compression, bending and shear loading. Both experimental and computational studies are conducted. For the experimental study, specimens made of scarf joints using carbon and glass woven fabrics are tested under compressive loadings to determine their joint failure strengths. Computational models are then developed to predict the joint strengths under the same conditions as in the experiments using the discrete resin layer model along with fracture mechanics and virtual crack closure techniques. The comparisons are good. Once the computational models are validated from the test results, the scarf joint strengths are computed under different loading conditions.

THIS PAGE INTENTIONALLY LEFT BLANK

TABLE OF CONTENTS

I.	INTRODUCTION	1
A.	BACKGROUND	1
B.	LITERATURE SURVEY	2
C.	OBJECTIVES	4
II.	FAILURE LOAD MODELING	5
A.	VIRTUAL CRACK CLOSURE TECHNIQUE (VCCT)	5
B.	MODIFIED VIRTUAL CRACK CLOSURE TECHNIQUE (MVCCT) ...	5
C.	VIRTUAL CRACK CLOSURE TECHNIQUE (VCCT)	7
D.	CRACK CLOSURE AND FAILURE CRITERIA	7
1.	Interactive Biquadratic Formulation	9
E.	CRACK GEOMETRY	9
III.	FABRICATION AND ANALYSIS OF SCARF JOINTS	13
A.	MATERIALS AND FABRICATION	13
B.	EXPERIMENTAL SETUP	15
C.	EXPERIMENTAL RESULTS	16
IV.	FINITE ELEMENT MODEL VALIDATION	23
A.	GLOBAL GEOMETRY	23
B.	LOADING AND CRITICAL LOCATION	25
1.	Model in Tension and Compression	25
2.	Model in Shear	26
3.	Model in Bending	26
V.	FEM VALIDATION FOR TENSION AND COMPRESSION	27
A.	RESULTS AND DISCUSSION	27
1.	Critical Locations	27
2.	Failure Load Results	28
a.	No Resin Interface	29
b.	With Resin Interface	30
c.	Angled Crack	34
B.	RESULTS FOR COMPRESSION MODEL	36
C.	SUMMARY	39
1.	Angled Crack Model	39
VI.	FEM TENSILE AND COMPRESSIVE LOADS	41
A.	TENSILE MODEL RESULTS	41
B.	COMPRESSION MODEL RESULTS	42
C.	INFLUENCE OF CARBON AND GLASS COMBINATIONS	45
VII.	ANALYSIS AND RESULTS FOR LOADING IN SHEAR	47
A.	ENERGY RELEASE RATE RESULTS	47
B.	SUMMARY	49
VIII.	ANALYSIS AND RESULTS FOR LOADING IN BENDING	51

A.	ENERGY RELEASE RATE RESULTS	51
B.	SUMMARY	52
IX.	MODE II MODELING OF CARBON AND GLASS COMPOSITES	53
X.	CONCLUSIONS AND RECOMMENDATIONS	57
	LIST OF REFERENCES	59
	INITIAL DISTRIBUTION LIST	61

LIST OF FIGURES

Figure 1.	Single and Double Scarf Joint. From [1].....	3
Figure 2.	Virtual Crack Closure Technique for Two-dimensional Solid Elements. From [2].....	6
Figure 3.	Deformed Crack Geometry—Without Resin Interface.....	10
Figure 4.	Crack Geometry—With Resin Interface.....	11
Figure 5.	Crack Geometry—Angled Crack in Resin Interface.....	12
Figure 6.	Geometry Showing Base and Patch.....	14
Figure 7.	Experimental Setup Using the Instron Instrument.....	15
Figure 8.	Compressive Tests—Joint Interface Failure.....	17
Figure 9.	Compressive Tests—Carbon Side Failure.....	17
Figure 10.	Experimental Compressive Results for all Three Experiments.....	19
Figure 11.	Stress Distribution—von Mises.....	20
Figure 12.	ANSYS Results Using Failure Criteria.....	21
Figure 13.	Experimental vs. FEM Prediction Under Compression.....	21
Figure 14.	Scarf Joint Dimensions.....	23
Figure 15.	Critical Location Without a Resin Interface.....	27
Figure 16.	Load Predictions—Model Without Resin Interface.....	30
Figure 17.	Load Prediction—Crack at Lower Interface.....	31
Figure 18.	Load Prediction—Crack at Resin Middle.....	32
Figure 19.	Load Prediction—Upper Resin Interface.....	33
Figure 20.	Load Prediction—18 Degrees Crack Along Resin Interface.....	35
Figure 21.	Load Prediction for 8:1 Taper Ratio Under Tension—9 Degrees Crack Along Resin Interface.....	36
Figure 22.	Failure Loads—4:1 Taper Ratio.....	38
Figure 23.	Failure Loads—8:1 Taper Ratio.....	38
Figure 24.	Load Prediction for 4:1 Taper Ratio Under Tension.....	41
Figure 25.	Load Prediction for 8:1 Taper Ratio Under Tension.....	42
Figure 26.	Scarf Joint in Compression.....	43
Figure 27.	Scarf Joint in Compression—4:1 Taper Ratio.....	44
Figure 29.	Model in Shear Showing Critical Locations.....	47
Figure 30.	Energy Release Rate—4:1 Taper Ratio.....	48
Figure 31.	Energy Release Rate—8:1 Taper Ratio.....	48
Figure 32.	Energy Release Rate—In Bending (4:1 Taper Ratio).....	51
Figure 33.	Energy Release Rate—In Bending (8:1 Taper Ratio).....	52
Figure 34.	Three-point Bending Modeling.....	53

Figure 35.	ANSYS Representation of Three-Point Bending von Mises Stress.....	54
Figure 36.	Energy Release Rate.....	55
Figure 37.	Failure Load Summary.....	56

LIST OF TABLES

Table 1.	Experimental Results for Glass/Carbon Joint.....	18
Table 2.	Properties of Carbon Laminate. From [3].....	24
Table 3.	Properties of E-Glass Laminate. From [5].....	24
Table 4.	Properties of Resin. From [6].....	24
Table 5.	Experimental Tensile Test Results (kN). From [3].....	29
Table 6.	Experimental Results for Glass/Glass Joint. From [3].....	37
Table 7.	Experimental Results for Carbon/Carbon Joint. From [3].....	37
Table 8.	Fracture Toughness and Failure Load.....	55

THIS PAGE INTENTIONALLY LEFT BLANK

ACKNOWLEDGMENTS

Professor Young Kwon for all his support and guidance during the course of my research and studies here at NPS.

Most of all to my family, mom and dad for their patience, understanding and support of my studies throughout my life.

THIS PAGE INTENTIONALLY LEFT BLANK

I. INTRODUCTION

A. BACKGROUND

The Total Ship Systems Engineering project at the Naval Post Graduate School has been geared towards the application and feasibility of using composite materials as a low maintenance alternative to metals, as well as a weight saving and radar absorption material. The U.S. Navy's push toward alternate materials (composites in this case) has caused a heightened interest in the study of carbon and glass laminates to replace metals in the superstructures of Navy ships. It is well known that composites save weight and thereby make the ships more fuel efficient or can be supplied with more weapons. Another advantage of composites is their low maintenance and resistance to corrosion. Of importance to the U.S. Navy are the effects caused by the external loading on the ships and the effects these loadings have on the composite materials as these could cause cracks to initiate and propagate. Another concern is the repairs and the effects of scarf joints might have on the superstructure's stiffness.

Scarf joints will mainly be used to attach two prefabricated sections or to repair an existing structure. The cost of the repair will depend on the size of the scarf joint needed to attach the new section of material.

Experimental testing is currently the best way to analyze scarf joints; however, it is also costly to perform. It is therefore the aim of this study to move towards a good model that is able to predict these failures with an improved understanding of the mechanics of the scarf joints.

B. LITERATURE SURVEY

Advancements in manufacturing, along with better process applications of composites—specifically, the application of carbon fiber in new technologies in the aerospace industry—have progressed tremendously, creating new challenges that must be overcome in order to make composites more reliable and affordable.

The objective of previous studies has been to examine the strength properties of a single and double-lap joint during a repair on a composite material and to optimize this patch in order to obtain the maximum residual strength by varying the major geometric properties.

Studies have been extensively conducted for composite laminates using two dimensional finite element analyses to identify critical areas with the use of computer modeling and experimental data. These and other works have focused on analyzing the influence of the overlap length on the joint's failure and critical areas. Experimental testing shows that delamination usually occurs along the resin layer [1]. Using a two dimensional model, Mahdi and Kinloch were able to model undamaged and overlap repaired scarf beams.

Using the commercial software ABAQUS, a two-dimensional model, a non-linear material, and a rectangular 8-noded finite element analysis were used under a tensile load on the repaired patch for the two cases shown below.

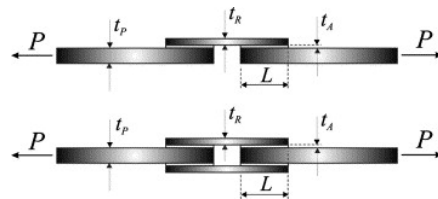


Figure 1. Single and Double Scarf Joint. From [1]

The study focused on five different points along the single lap joint to include the top, middle and bottom of the adhesive (resin), the adherent and the patch. The joint strength was studied using ABAQUS on a mix-mode damage model, which helps model crack initiation and growth. The crack was analyzed by gradually reducing the mechanical and fracture properties of the composite material along the joint in order to identify the values that would cause delamination within the layers.

The study shows the highest shear distribution at the bottom and top interface of the adhesive, which means that the failure will most likely occur at one of these interfaces. Peel delamination stresses are higher in single-lap joints due to bending. In the instance where the patch is thicker, the stiffer it will become and thereby decreasing the deformity and bending moment.

C. OBJECTIVES

This study is to compare the joint strengths of scarf joints made of different composite material combinations like glass/glass, glass/carbon, carbon/glass, and carbon/carbon under various loading conditions; tension, compression, bending and shear loading. To this end, computational models are developed based on a discrete resin layer model. In order to predict the joint interface strength, fracture mechanics is applied with a virtual crack closure technique. The computational models are validated against experimental data for compressive loading. The validated numerical models are then used to evaluate the scarf joint strengths under different loading conditions.

II. FAILURE LOAD MODELING

A. VIRTUAL CRACK CLOSURE TECHNIQUE (VCCT)

The virtual crack closure technique (VCCT) is a method used to extract Mode I and Mode II components of energy release rates from finite element fracture models. Two techniques were explored for this study, the Virtual Crack Closure Technique (VCCT) and the Modified VCCT. The modified VCCT was found to give better results and resulted in a significant time saving while running the models in ANSYS. For this reason, the modified VCCT is at the center for this study.

B. MODIFIED VIRTUAL CRACK CLOSURE TECHNIQUE (MVCCT)

The modified VCCT approach shows potential as a consistent method of extracting crack extension modes. It uses the same information from a finite element analysis (i.e., nodal forces and displacements) as the traditional VCCT method does. The VCCT to extract modes of crack extension is studied for cases of a crack along the interface between two in-plane orthotropic materials.

This process has its advantage over the traditional VCCT as only one FEM solution has to be generated. This in itself can save ample of time. This method was compared to the traditional VCCT and obtained the result that was compared better to experimental results. It was therefore decided to continue using this process and specified where it was used.

When using the Modified Crack Closure Technique the elements must be equal in size to the length Δa , as shown in Figure 2 and 5. Also, when using this method, it is assumed that this extension will not considerably change or alter the crack tip as the elements deform [2]. Since the deformations were small, this was satisfied throughout the analysis.

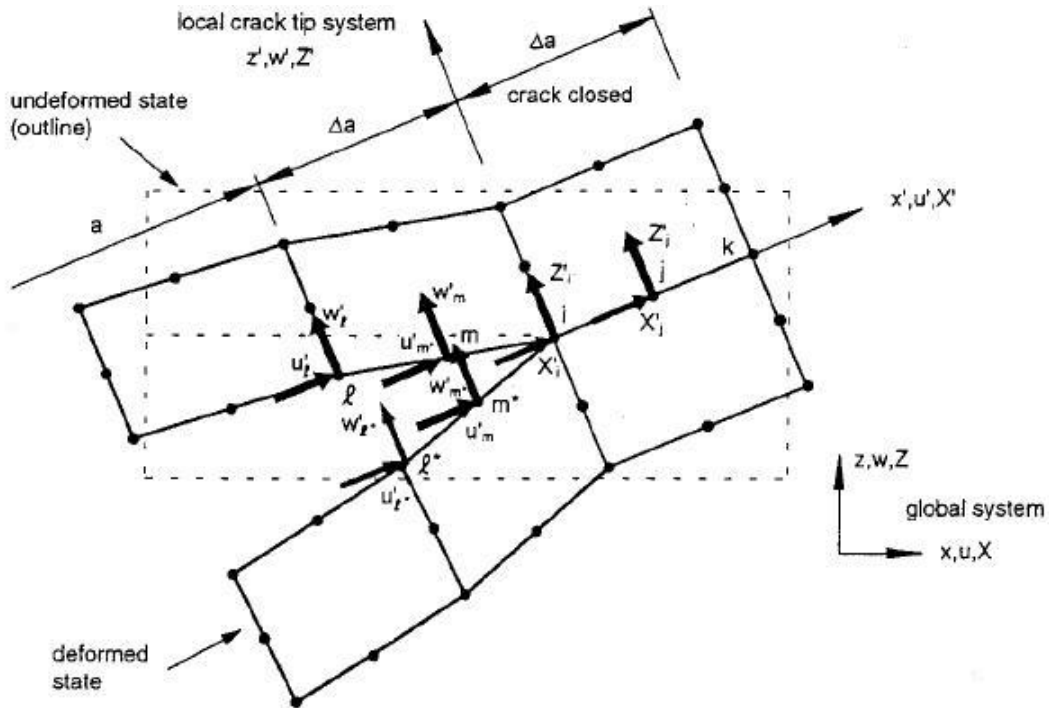


Figure 2. Virtual Crack Closure Technique for Two-dimensional Solid Elements. From [2]

In calculating the energy release rates for Modes I and II, G_I and G_{II} , the following formulas were used for this one-step method following Figure 2 terminology:

$$G_I = \frac{-\left[Z_i (w_l - w_{l^*}) + Z_j (w_m - w_{m^*}) \right]}{(2\Delta a)} \quad (1)$$

$$G_{II} = \frac{-\left[X_i (u_l - u_{l^*}) + X_j (u_m - u_{m^*}) \right]}{(2\Delta a)} \quad (2)$$

When running the analysis in ANSYS, the element mesh size must be made to equal Δa in order to use this model. For this specific process, the forces and displacement acting on the crack must be taken along the crack's axis. This requires the placement of a local axis along the fracture path.

C. VIRTUAL CRACK CLOSURE TECHNIQUE (VCCT)

Modes I and II can also be easily calculated using this method, however, this requires a two-step analyses. The first step requires the forces to be obtained at the crack tip while it is still closed. In the second step, the crack is opened by (in this case) to 5% and the displacements obtained at the same location where the forces were calculated. The traditional Crack Closure Technique is best described in "The Virtual Crack Closure Technique: History, Approach and Applications" by Krueger [2].

D. CRACK CLOSURE AND FAILURE CRITERIA

Through the use of the previous methods described above, the Energy Release Rates can be calculated. Along with using the force applied to the specimen and the

critical energy release rates, the fracture failure criteria equations were provided by Green [3]. These equations, equation (3) through (5), are used to calculate the failure loads for each of the specimens.

Mixed Linear

$$P_{fail} = \frac{1}{\sqrt{\frac{G_{Ic}G_{II} \text{ applied} + G_{IIc}G_I \text{ applied}}{G_{Ic}G_{IIc}P_{\text{applied}}^2}}} \quad (3)$$

Mixed quadratic

$$P_{fail} = \frac{1}{4 \sqrt{\frac{G_{Ic}^2G_{II}^2 \text{ applied} + G_{IIc}^2G_I^2 \text{ applied}}{G_{Ic}^2G_{IIc}^2P_{\text{applied}}^4}}} \quad (4)$$

Interactive Biquadratic

$$P_{fail} = 4 \sqrt{\frac{1}{\frac{G_I^2 \text{ applied}}{G_{Ic}^2} + \frac{m G_I \text{ applied} G_{II} \text{ applied}}{G_{Ic} G_{IIc}} + \frac{G_{II}^2 \text{ applied}}{G_{IIc}^2}}} \quad (5)$$

All three equations were explored in order to find the best fit for the model. These results are provided in the following sections.

1. Interactive Biquadratic Formulation

The interactive criterion as described in Green's report [3] provides the best results, which are comparable to the experimental results. This equation, equation (5), can be modified through the variable "m," which controls the amount Mode I and II interact. For this report, a value of -1.3 was used throughout giving results within range of the experimental results as described in the following sections.

E. CRACK GEOMETRY

Cracks of several shapes and sizes are explored for the different models used. The starting crack was assumed to be of an "undetectable" length of 0.0254 cm (0.01 in) using an element crack extension of 5%, i.e., Δa set to 0.00127 cm. Different kinds of cracks were considered to determine what kind of crack was the best to produce the result matching the experimental data. The crack was initially applied to the model creating a discontinuity between the composite materials layers, and using four-noded elements it was allowed to deform. The crack was then extended by 5% of the initial crack. The crack was created using twin nodes that were not connected, but allowed to move independently of each other. The crack is only connected by a single node at the crack tips, and the length and extension was initially modeled on the scarf joint without resin, as shown below in Figure 3.

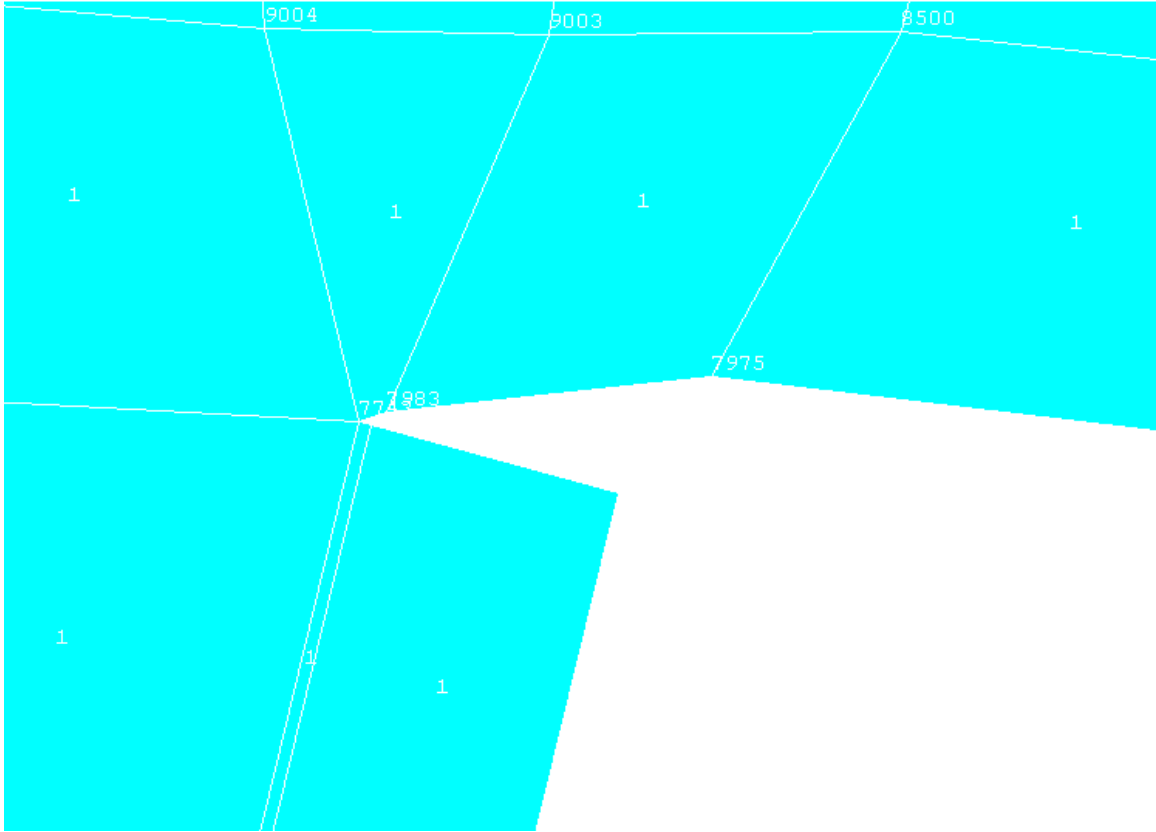


Figure 3. Deformed Crack Geometry—Without Resin Interface

This crack geometry was also used to model the crack on the model with resin and conducted in three separate phases as seen in Figure 4. This was applied on bottom resin/composite layer, to the middle of resin and on the top interface of resin/composite layer; and analysis conducted.

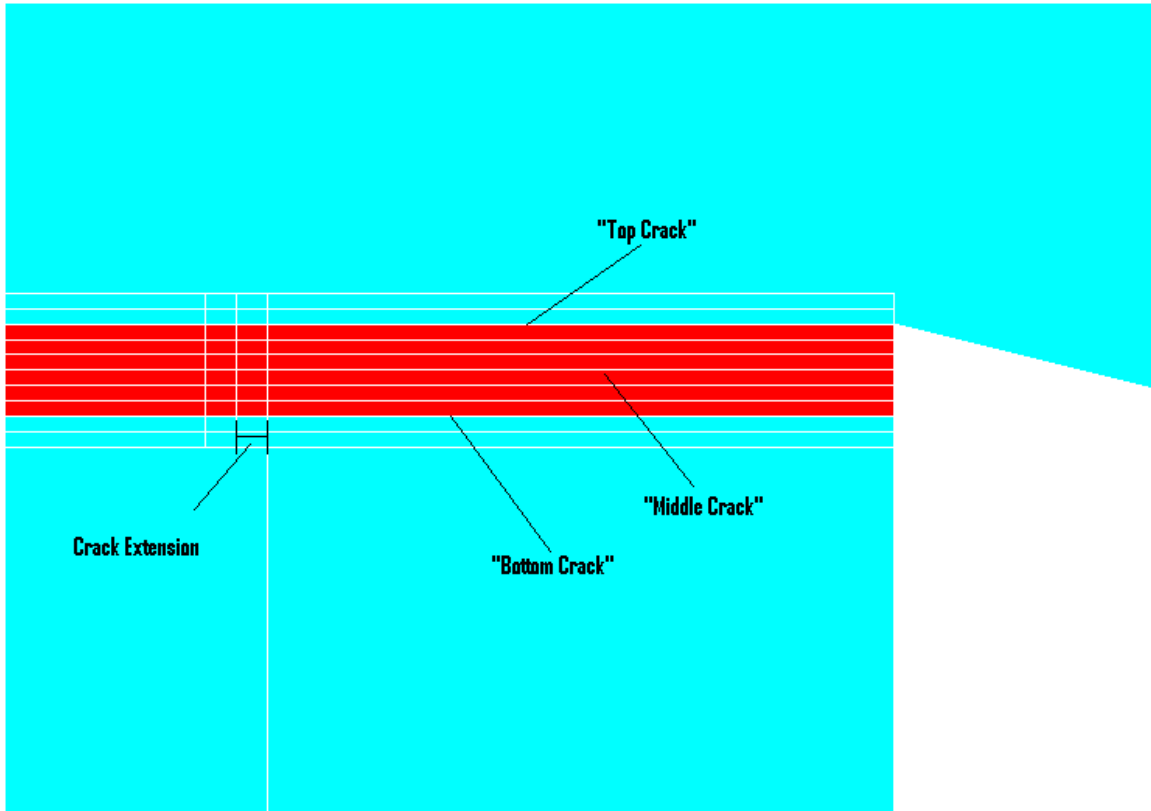


Figure 4. Crack Geometry—With Resin Interface

For the third model with resin interface and 4:1 scarf ratio, a slanted crack was modeled where the taper ratio of the scarf is taken into account when creating the crack. This crack was created to match the slope generated by the scarf joint. In this case, the slope angle is 18 degrees, as shown on Figure 5.

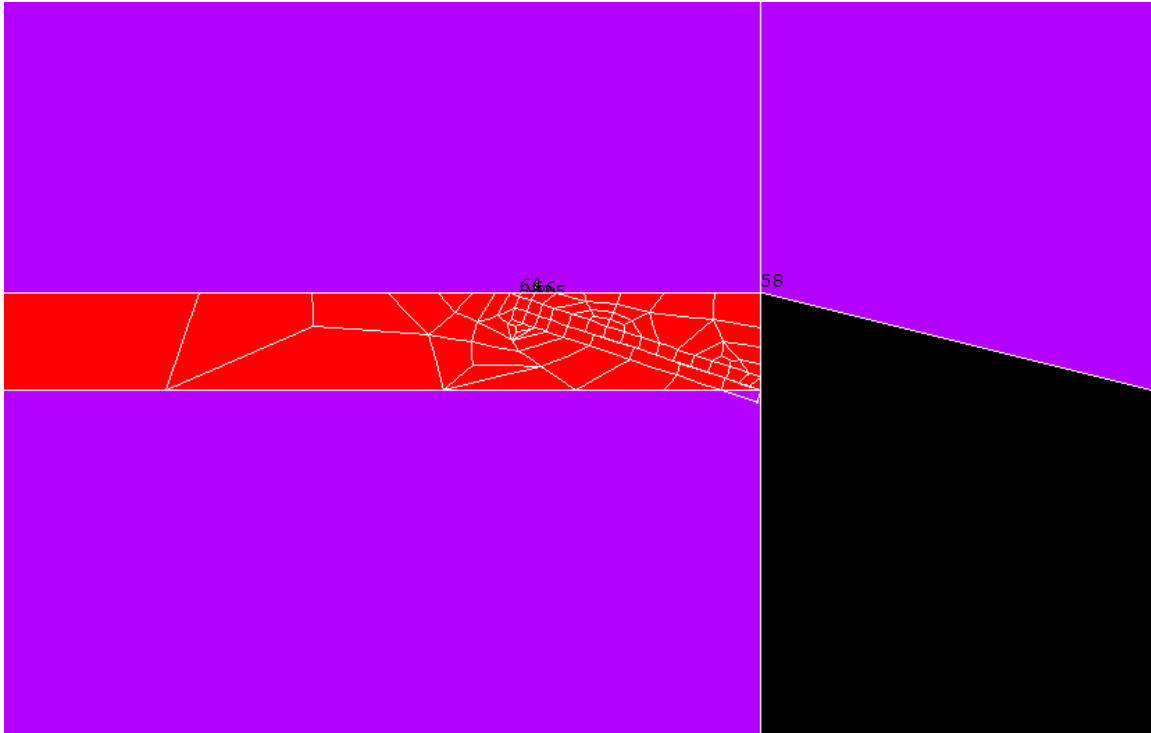


Figure 5. Crack Geometry—Angled Crack in Resin Interface

The fourth model has a taper ratio of 8:1 giving a crack angle of 9 degrees. For the tapered cracks, only one crack was modeled. This crack was assumed to originate at the interface bottom of resin/composite, as shown in Figure 4.

The tapered cracks modeled tend to be of a smaller length since the resin was approximately 0.05 mm in thickness and would otherwise cut into the composite layers. Because of these smaller cracks, the second model was recalculated (Fig. 4) using horizontal cracks that match the length of the tapered cracks.

III. FABRICATION AND ANALYSIS OF SCARF JOINTS

In order to understand the mechanics of scarf joint failures, experimental results were conducted. These experiments include the construction of glass and carbon woven fabric laminate joints and analyzed under compression.

A. MATERIALS AND FABRICATION

In the fabrication of these specimens, the VARTM process was used throughout. This is a deviation from previous analysis where the hand lay-up was applied. This difference is seen in the thickness of the samples where a thickness of 0.940 cm could be expected for carbon fiber using the hand lay-up [3]. This is in contrast to an approximate thickness of 0.564 cm using the VARTM process for the same amount of sheets of carbon fibers.

Another difference seen in these specimens is the relative difference in thickness between carbon and glass fiber when combined to create the joint. Total 16 layers were used to create the carbon side for the joint whereas only 12 layers of glass fiber were used. This was done in order to balance the difference in thickness of both materials. This was also done knowing that the joint might be weaker on the glass side.

The main cause of why these samples were thinner than previous specimens was the use of a negative pressure of 12 psi (84.6 kPa) thereby putting a lot of force on the fibers as well as getting rid of any air inclusions. This high

vacuum highly compressed the fibers creating the thinner sample and the possibility that a specimen this thin might buckle under compressive loads.

Three different samples were created for this experiment using two procedures. The first of the samples consisted of glass as the base and carbon as the patch as shown in Figure 6. For this study a combination of Carbon (as the base) and Glass (as the patch) will be referred by Carbon/Glass and vice-versa.

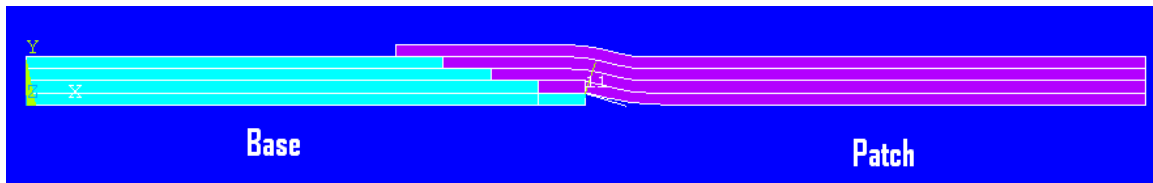


Figure 6. Geometry Showing Base and Patch

The carbon side of the joint was first created and cured for 72 hours before sanding down the joint in preparation for creating the second half of the joint with glass fiber.

After both sides were joined and let to cure for another 72 hrs, the samples were cut to a size of 9 in (22.86 cm) by 1.5 in (3.81 cm).

This same method was applied for the scarf joint consisting of carbon as the base and glass as the patch. However, a third joint was created consisting of carbon as the base and glass as the patch, but instead of creating each separately, both were created as a single set for comparison.

B. EXPERIMENTAL SETUP

The experimental setup consisted of using the Instron 4507 apparatus. The experiments were setup, as shown in Figure 7.



Figure 7. Experimental Setup Using the Instron Instrument

The specimens were placed under a compressive load until failure. Both force and displacement were recorded by the affixed computer using Instron software (Version 8.15.00). High forces were expected and therefore a head of a higher load rating (up to 200kN) was used for the experiment.

In order to apply an even distribution of the forces along the end of the specimen, a flat surface is required. Since the vices holding the specimen did not have a flat surface, two flat metal plates were used to accomplish this task, as can be seen from Figure 7. A total six samples were tested for each of the three different joint.

C. EXPERIMENTAL RESULTS

All samples were measured and compared to each other for differences in areas since two processes were used in creating the samples.

From the results, some observations can be concluded from the 18 samples tested:

1. For the Glass/Carbon joint, one of six samples failed through the joint interface, as shown in Figure 8, producing the highest failure load. These results are shown in Table 1.

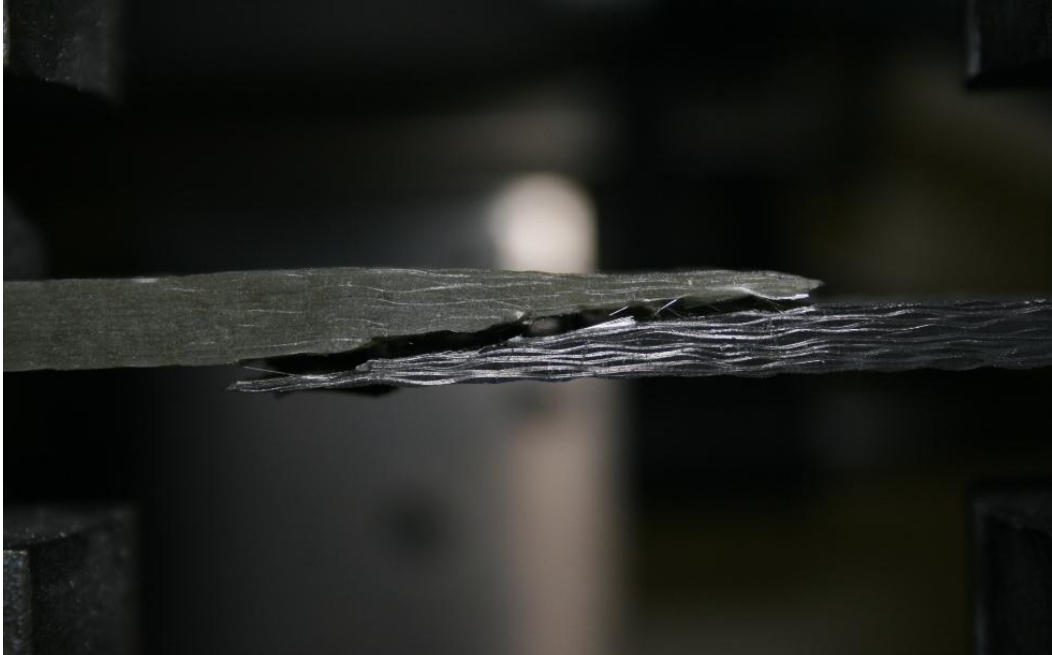


Figure 8. Compressive Tests—Joint Interface Failure

The other six samples failed through the carbon section near the bottom layer tip of the glass fiber as shown in Figure 9.



Figure 9. Compressive Tests—Carbon Side Failure

Table 1. Experimental Results for Glass/Carbon Joint

Sample #	Fail Load (kN)
1	25.24
2	25.64
3	29.53
4	31.64
5	30.76
6	33.98
7	33.79
Avg	30.08285714
STDV =	3.542874136

2. In the Carbon/Glass analysis, two samples failed through the joint interface (Figure 8), and two failed through the carbon section as in Figure 9. These last two samples that failed through the joint interface had a greater strength than the two that failed through the carbon section, which indicates that when we have straight carbon layers, there is an increase in the failure strength under compression.

3. In the one-step curing process for the Carbon/Glass, three samples failed through the joint interface (as shown in Figure 9), which produced less strength than the two samples that failed on the carbon side.

4. The two-step cure process for Carbon/Glass composite shows a greater strength than the two-step cured Glass/Carbon. The Carbon/Glass combination had an average of 39kN fail load compared to a 30kN load for the one-step process as shown in Figure 10.

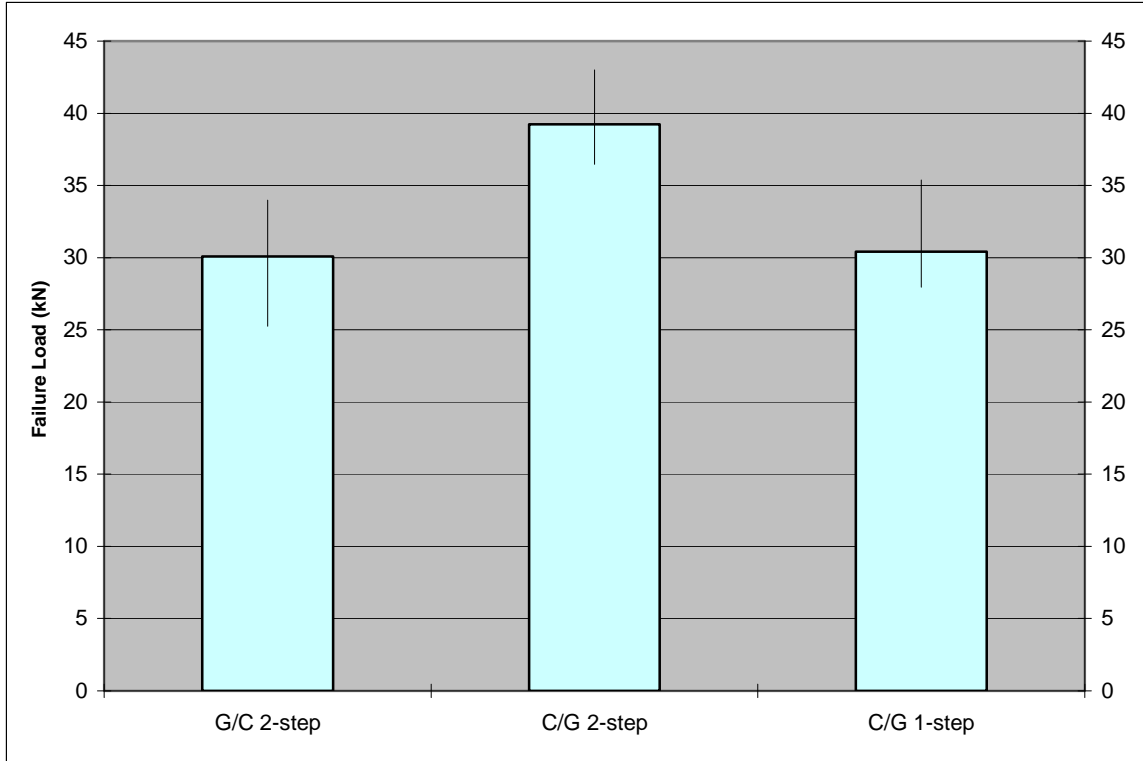


Figure 10. Experimental Compressive Results for all Three Experiments

A new computer model had to be generated to match the dimensions of the fabricated models. These models were also created as isotropic with a resin interface layer at the local model and a slanted crack built-in as an assumed propagation path as described in this study. This crack is assumed to propagate along the joint where the stresses are concentrated as shown in Figure 11.

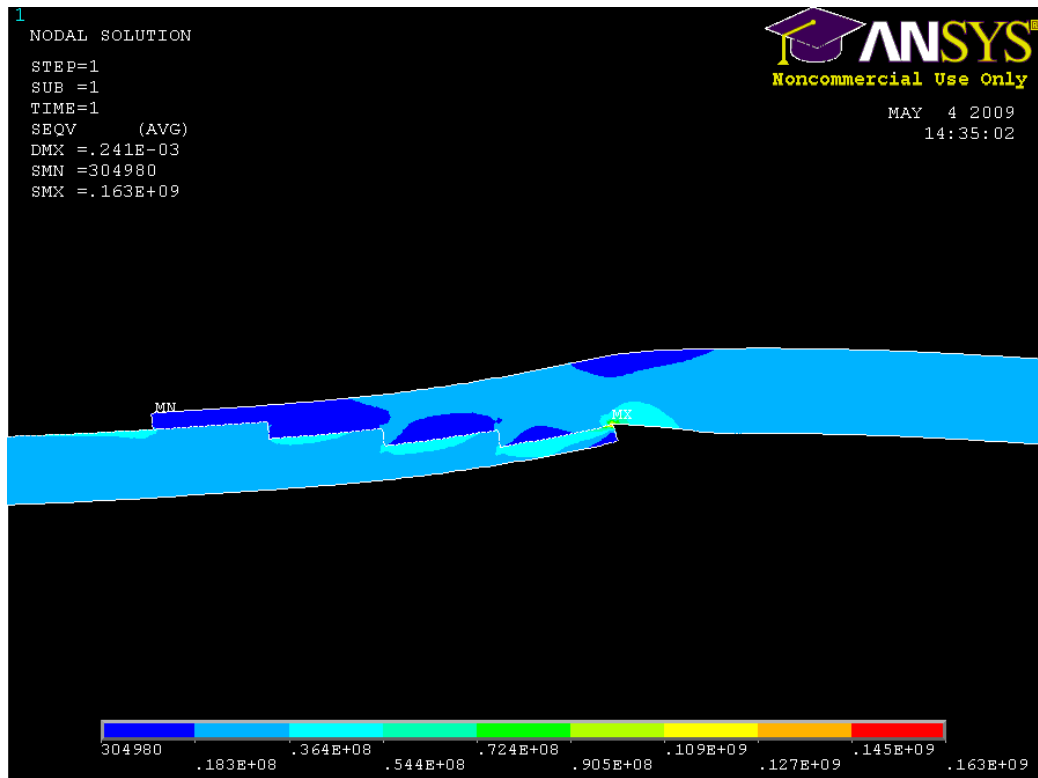


Figure 11. Stress Distribution–von Mises

In predicting the failure loads, the Mix Linear, Mixed Quadratic and Interactive Biquadratic failure criteria were used and are shown in Figures 12 and 13.

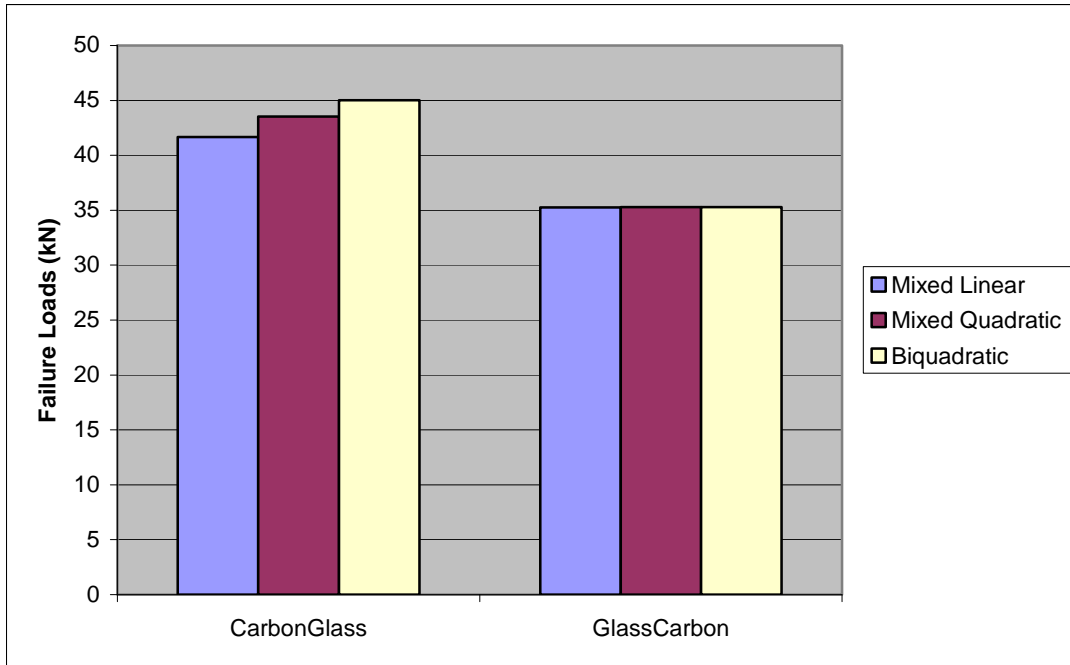


Figure 12. ANSYS Results Using Failure Criteria

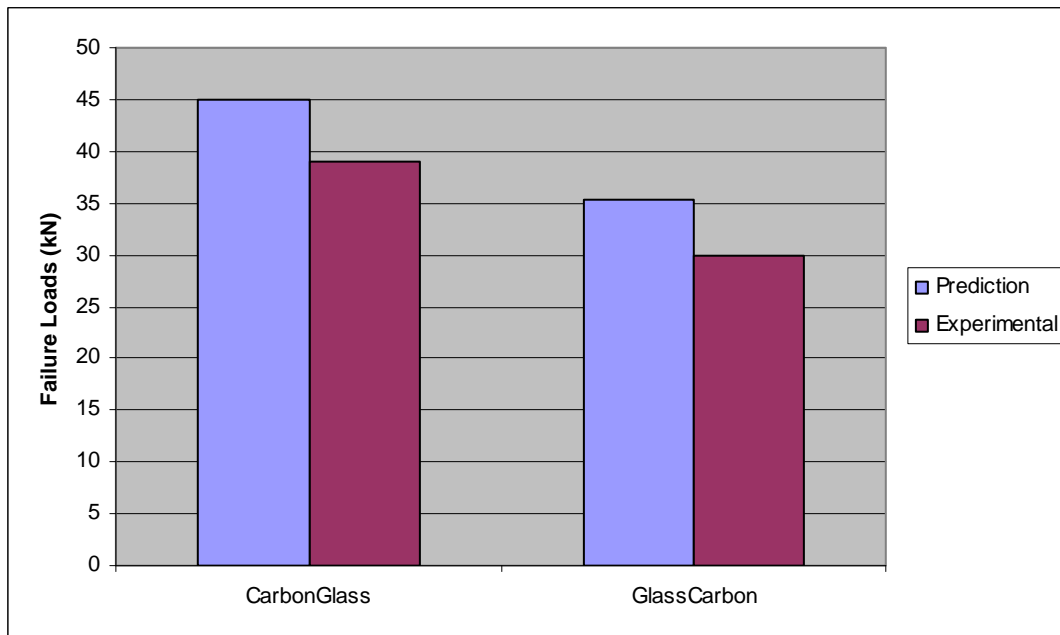


Figure 13. Experimental vs. FEM Prediction Under Compression

There was not much difference in the results obtained, however, the Interactive Biquadratic, with a variable "m" of -1.3, provided the best results compared to the experimental analysis. This model overestimated the failure with a 14% error.

IV. FINITE ELEMENT MODEL VALIDATION

A. GLOBAL GEOMETRY

For the purpose of this study and in order to validate experimental results obtained from NSWCCD, the models' geometry was based on the test specimens from NSWCCD. These specimens consisted of solid laminate plates created with a scarf of length L at the center. These specimens were 9.525 cm by 22.86 cm with a thickness of 0.968 cm as shown in the following figure, and consist of four-ply thickness using 16 plies total for each side of the model.

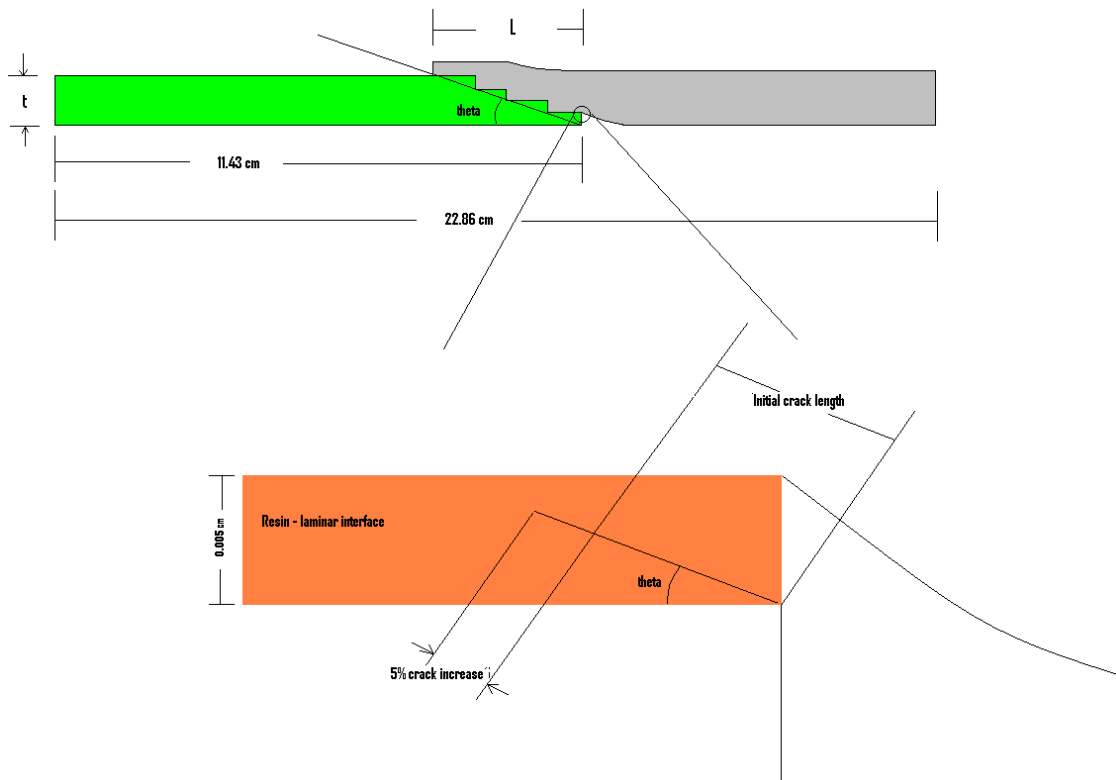


Figure 14. Scarf Joint Dimensions

The models consisted of either 16 plies of 24 *oz/yd*² E-glass woven-roving and/or 16 plies of Toray T700 carbon fiber along with Dow Derakane 510A vinyl ester resin. Tables 2 through 4 state the properties of these materials.

Table 2. Properties of Carbon Laminate. From [3]

Property		Value	Units
Modulus	E	52.4	GPa
Poisson's Ratio	ν	0.34	
Shear Modulus	G	3.79	GPa

Table 3. Properties of E-Glass Laminate. From [5]

Property		Value	Units
Modulus	E	17.23	GPa
Poisson's Ratio	ν	0.24	
Shear Modulus	G	6.62	GPa

Table 4. Properties of Resin. From [6]

Property		Value	Units
Modulus	E	8.34	GPa
Poisson's Ratio	ν	0.28	
Shear Modulus	G	3.24	GPa

B. LOADING AND CRITICAL LOCATION

Varying loading patterns were applied to the models. The global model was fixed at the far left end while the loads were applied at the far right. The model was subjected to tension, compression, shear and bending.

1. Model in Tension and Compression

The models were fixed in both directions of their left ends while they were displaced by ± 0.02431 cm in the axial direction and fixed in the transverse direction at their right ends. In order to find the applied equivalent force, the forces at each node on the far right end were summed using ANSYS tools. This value would vary depending on the scarf configuration. The sum of the forces resulted in a lesser value when glass fiber was applied to the right end as it is more flexible than carbon.

Through testing, as well as observing the models, the critical location is found to be at the ends at the ply termination at both ends of the scarf. For a scarf joint, the resin acts as an adhesive. It is also the weakest point as its strength is much lower than glass or carbon fiber.

For the case of this model, the most critical area is found to be at the bottom ply termination where the two plies meet. Due to the model's geometry, a corner is found at this location creating a stress amplifier. For this reason, a local area is created around this location and the focus is placed here.

As the model is placed in tension or compression, a bending moment results at the center of the scarf creating increased stress that affects the critical location.

2. Model in Shear

For the shear model, a displacement of ± 0.02431 was applied in the transverse direction. This again created a bending moment at the critical location of the scarf joint on the bottom side of the sample. The sample was only tested with a displacement in the upward transverse direction as this resulted in the worst case scenario.

3. Model in Bending

The last loading configuration was a 1 kN-m moment CCW applied at the far right end of the model while the left end remained fixed in all axes. This, just like the shear model, bending created a stress at the critical spot.

V. FEM VALIDATION FOR TENSION AND COMPRESSION

In order to create a working model and be able to use this to calculate varying loading conditions, it must first be validated by comparing experimental results obtained from Green [3] and Slaff [4] and compared to the model's solution. This process and results are as follows.

A. RESULTS AND DISCUSSION

1. Critical Locations

The cracks considered for the models were created at the lower scarf joint where the two stacks of layers meet. The interface at the critical location found through an analysis without any crack using the von Mises strain plot as shown on Figure 15.

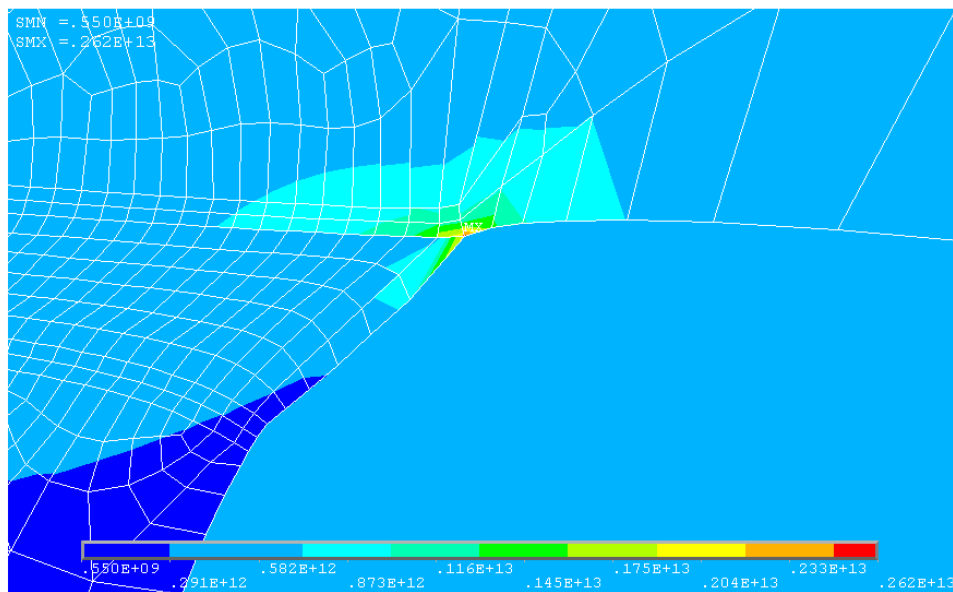


Figure 15. Critical Location Without a Resin Interface

At this specific area a crack was inserted and analyzed using the two-step and one-step method of the Virtual Crack Closure Technique as described in the previous sections.

The force applied in the +x-direction on the model is transferred from the patch (right side) to the parent structure (left side) through the resin layer. The stress at the critical location is augmented by the moment created due to the geometry of the model and due to the fact that it is not allowed to displace in the y-direction at either end. The crack growth occurs due to the shear created between the upper and lower terminal surface ply as well as a crack opening due to the stress created by the bending. Both Modes I and Mode II were present on each of the models.

Using fracture criteria along with the Virtual Crack Closure Technique, failure load predictions were calculated for Glass/Glass.

2. Failure Load Results

The experimental results used for comparison were obtained from testing conducted Naval Warfare Center, Carderock Division and shown in Table 5.

Table 5. Experimental Tensile Test Results (kN).
From [3]

	Scarf (0.968, 4:1)	Scarf (0.968, 8:1)
	115.7	146.8
	151.2	160.1
	146.8	142.3
	97.9	173.5
	84.5	213.5
	111.2	155.7
	129	146.8
	137.9	173.5
	133.4	177.9
		155.7
		146.8
		142.3
		164.6
		146.8
Average	123.1	160.5

a. No Resin Interface

Initially the specimens were modeled without a resin interface as in Figure 15. And, as in Figure 15, the forces were shown to work in shearing as well as opening of the crack. Failure loads are shown in Figure 16, which were calculated using equations (3) through (5).

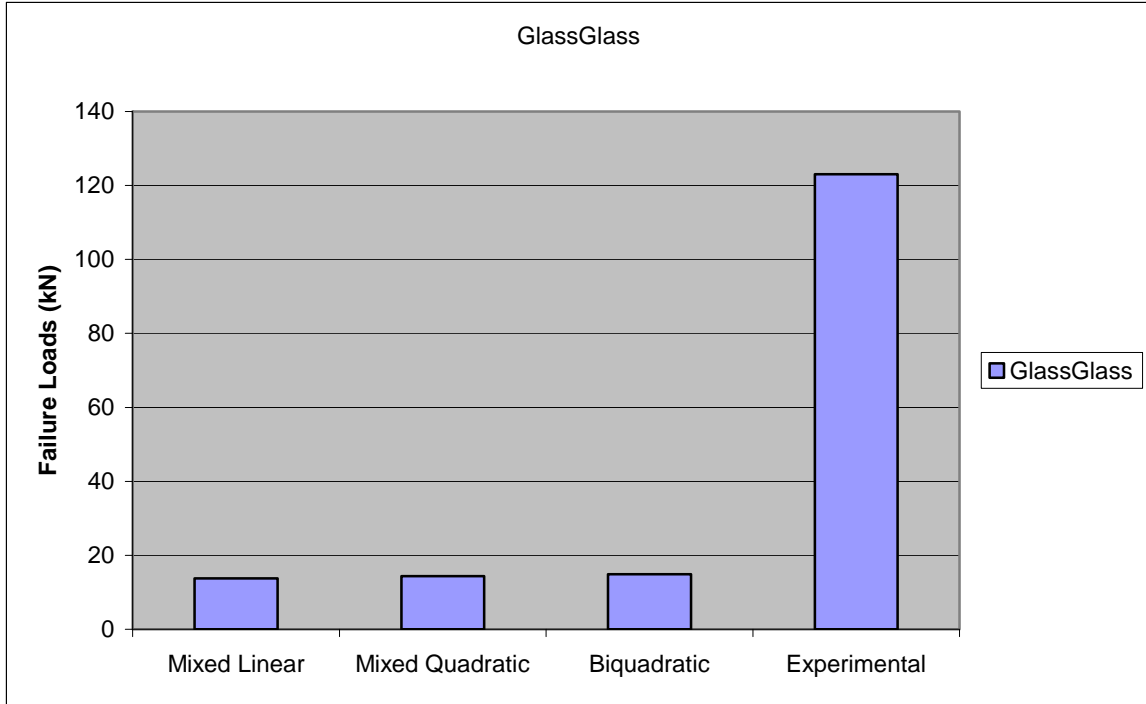


Figure 16. Load Predictions—Model Without Resin Interface

These results for the Glass/Glass composite were compared to the experimental results for validation of the model. In the case where there is no resin interface, these results were not consistent with the expected results as seen from the previous graph.

b. With Resin Interface

Figures 17 through 19 show the models containing cracks on bottom, middle and top of resin interface. These results, however, are not entirely validated by the experimental results. The results for the top crack were in close proximity to the experimental results and were off by 40% of the average experimental results.

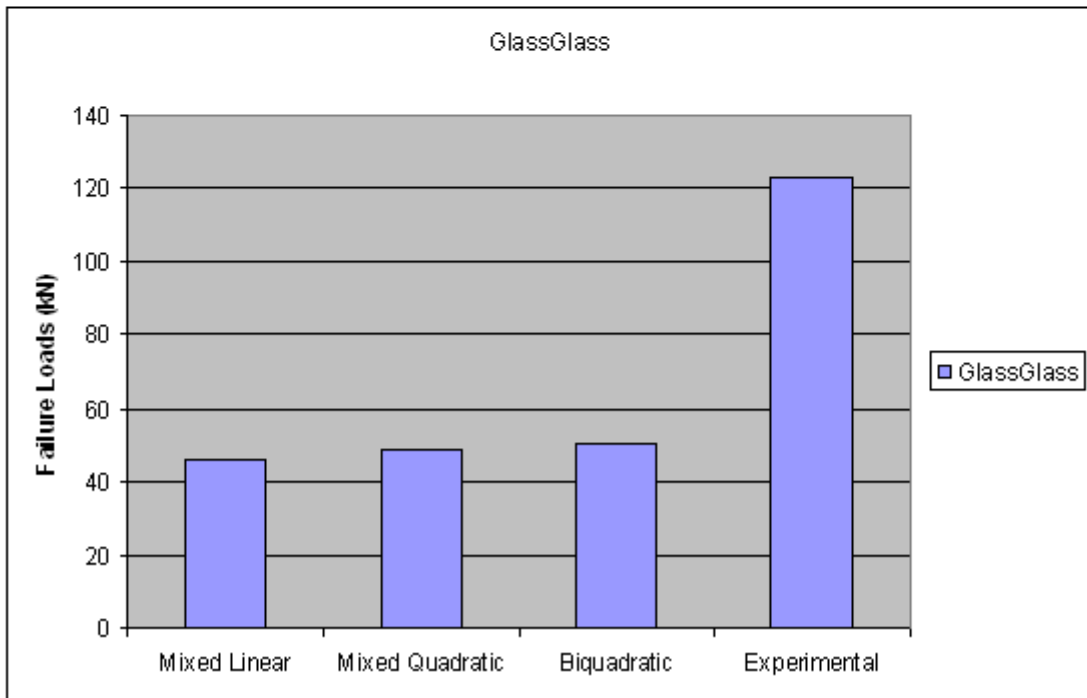
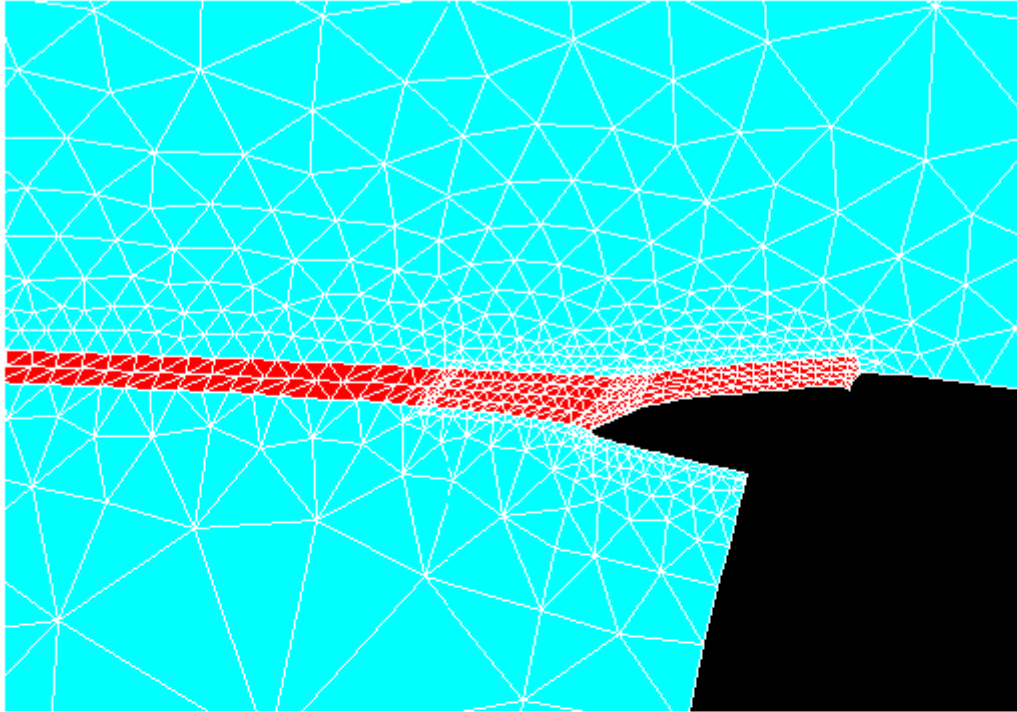


Figure 17. Load Prediction—Crack at Lower Interface

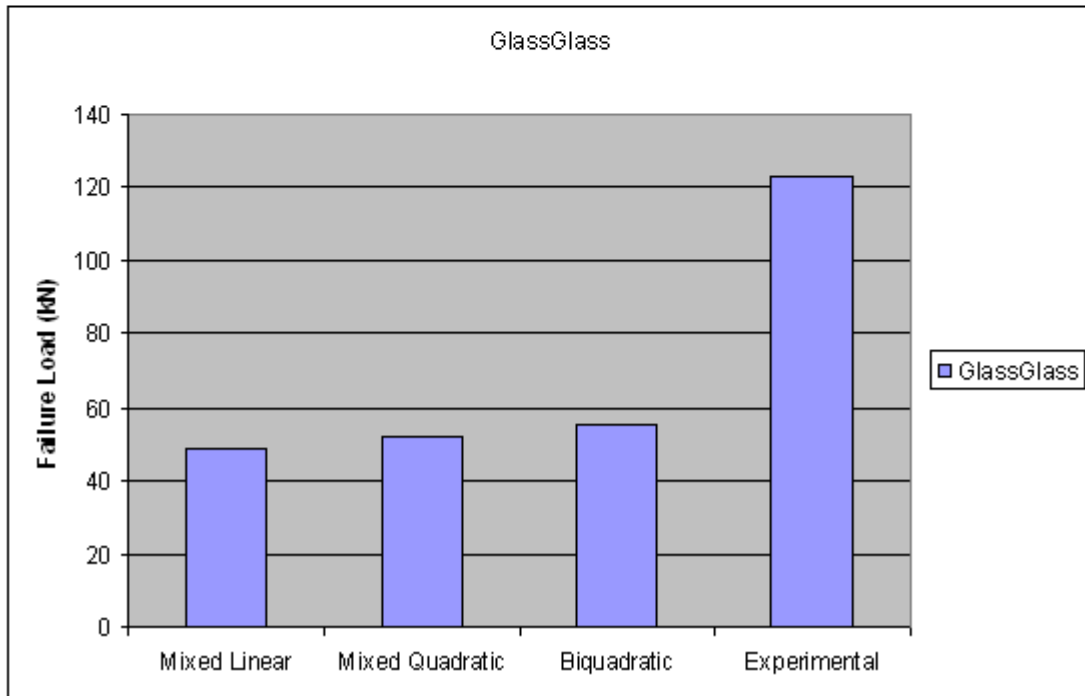
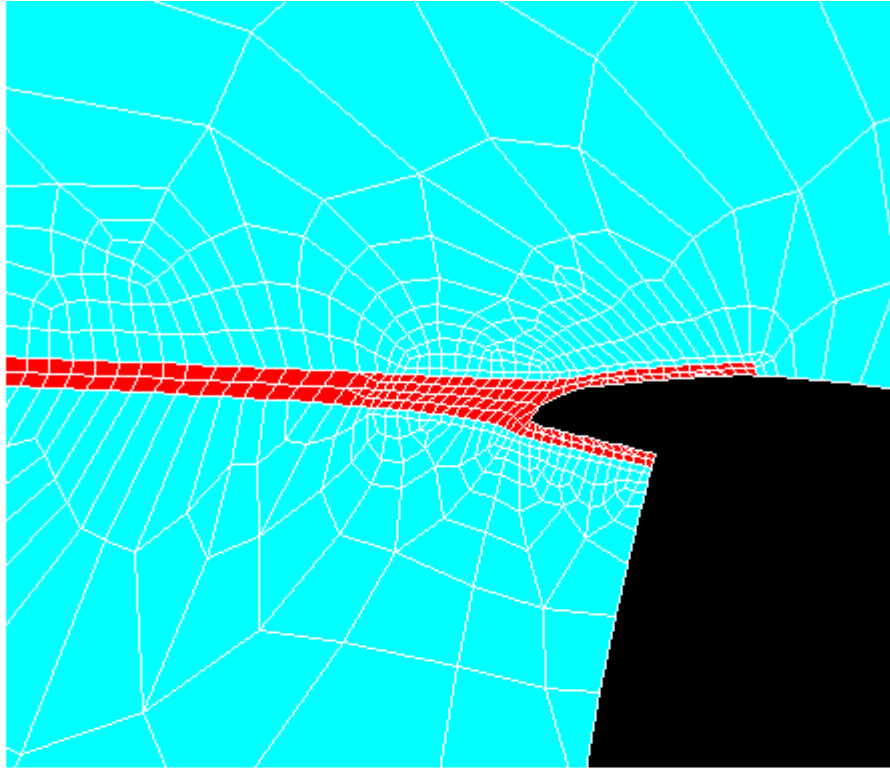


Figure 18. Load Prediction—Crack at Resin Middle

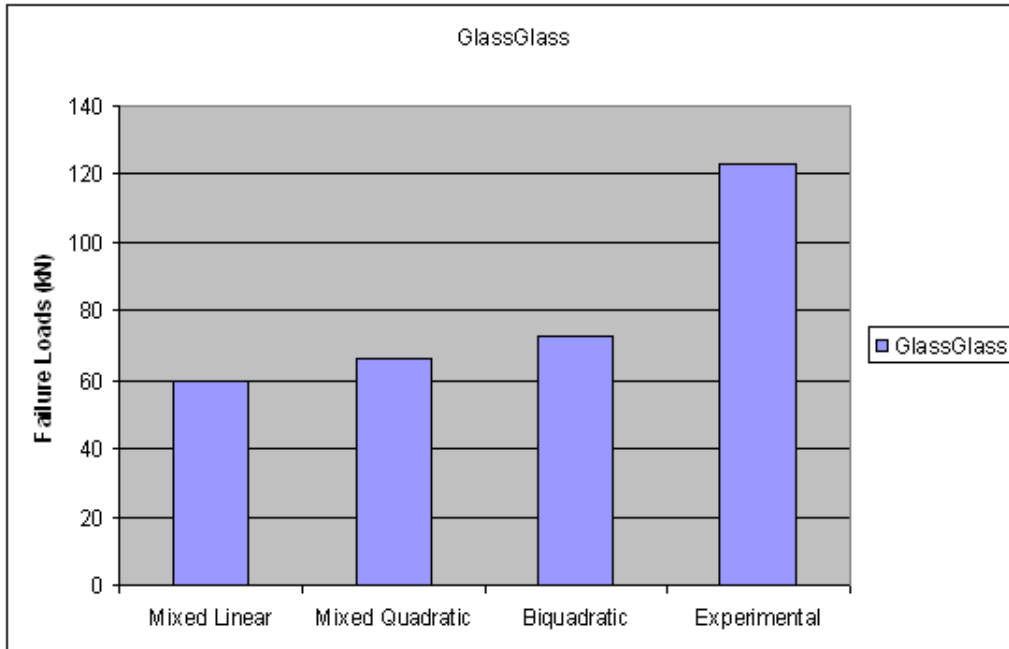
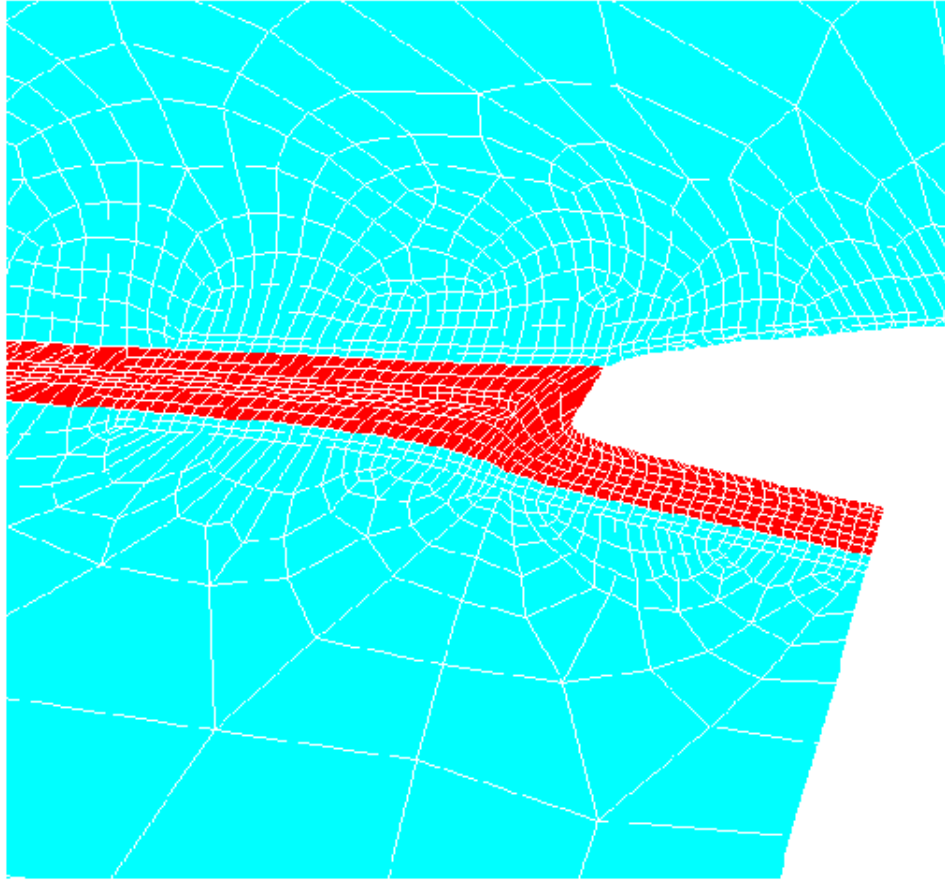


Figure 19. Load Prediction—Upper Resin Interface

c. Angled Crack

For the case of the angled crack, a separate local coordinate axis must be applied. Because the crack is angled, it is modeled to be smaller than the horizontal cracks since the resin interface is only 0.005 cm thick and the crack will not propagate through the composite layer.

The results obtained through the use of the angled crack proved to provide the best comparable results to the experimental values. The results are shown in Figures 20 and 21. Through the use of the Interactive Biquadratic equation, and an "m" value of -1.3, an error of 6% was found. The Mixed Quadratic produced an error of 34%, whereas the Mixed Linear gave a 44% error. From the analysis conducted, all three equations were conservative and under predicted the load failure.

The model is validated for the case where the specimen is made entirely of glass fiber with resin interface. Unfortunately, there is no experimental data to validate the other cases where the composites are alternated between carbon and glass and more testing is required.

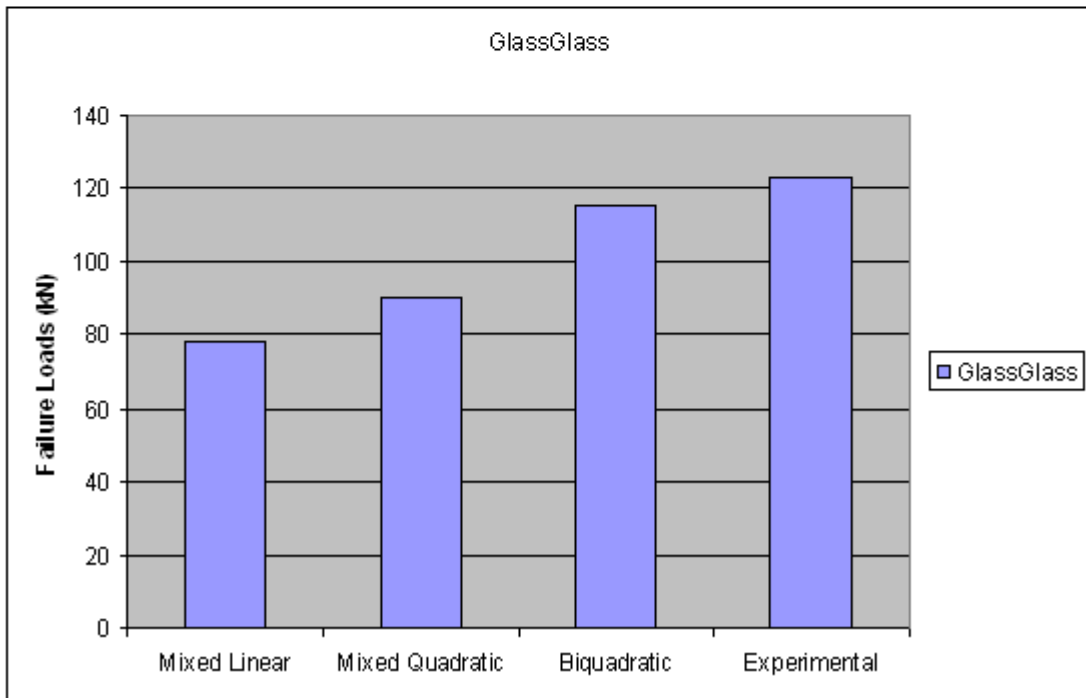
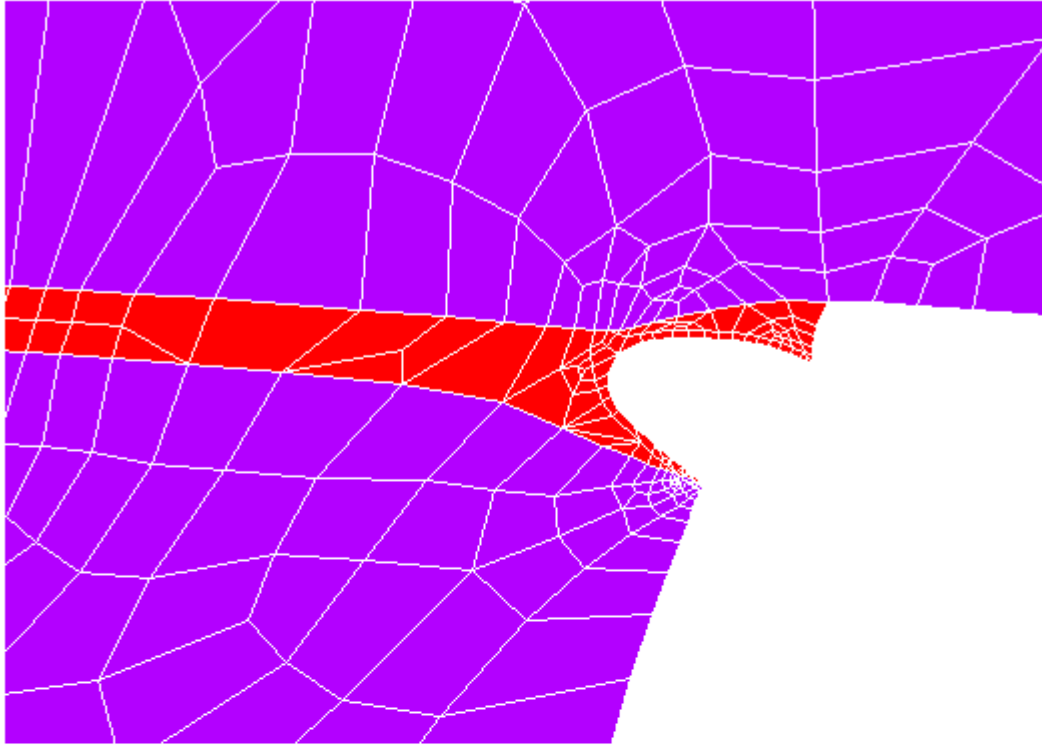


Figure 20. Load Prediction—18 Degrees Crack Along Resin Interface

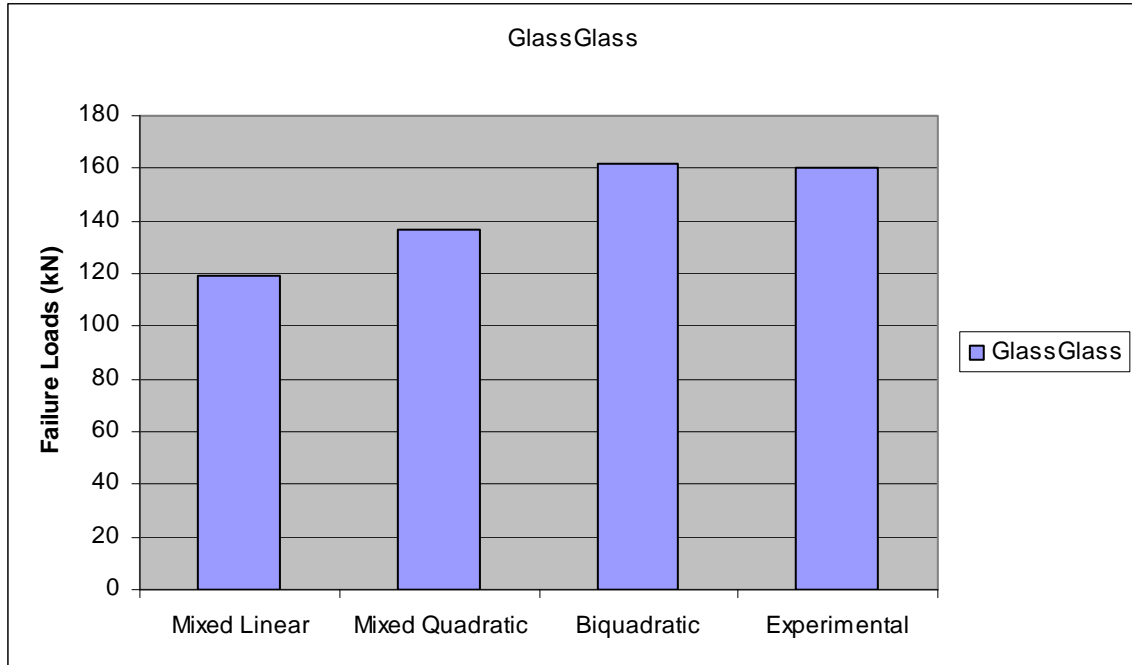


Figure 21. Load Prediction for 8:1 Taper Ratio Under Tension-9 Degrees Crack Along Resin Interface

B. RESULTS FOR COMPRESSION MODEL

Using the same models as before, compressive loads are applied to the glass/glass and carbon/carbon samples of 4:1 and 8:1. These results are compared to the experimental data shown in Tables 6 and 7 and plotted in Figures 22 and 23.

Table 6. Experimental Results for Glass/Glass Joint.
From [3]

	Scarf(.968, 4:1)	Scarf(.968, 8:1)
	-84.5	-71.2
	-84.5	-80.1
	-84.5	-129
	-93.4	-102.3
	-84.5	
	-80.1	
	-89	
	-97.9	
	-84.5	
	-89	
Avg	-87.19	-95.65

Table 7. Experimental Results for Carbon/Carbon Joint.
From [3]

	Scarf (.968, 8:1)
	-179.466
	-154.948
	-177.459
	-170.449
	-174.278
Avg	-171.32

The results obtained in the validation model are in the 3% range for the Carbon/Carbon and 25% off for the Glass/Glass case. It should be noted that these last values from Table 6 (8:1 taper ratio), the specimens consistently buckled under the compressive load and are for the most part unreliable.

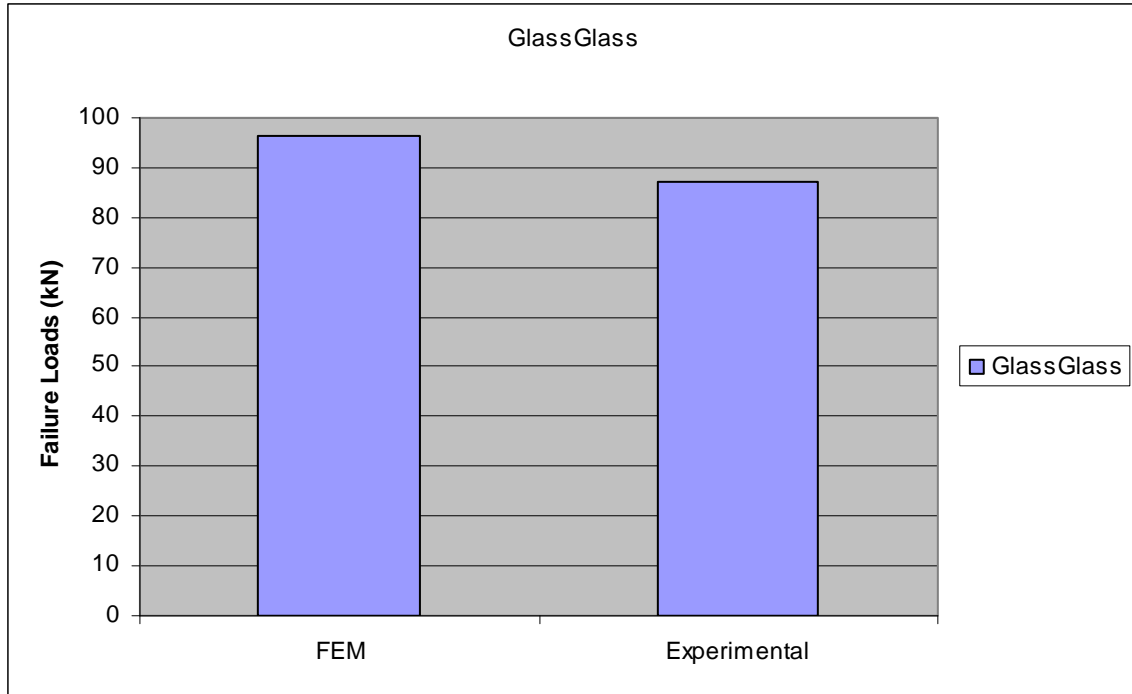


Figure 22. Failure Loads-4:1 Taper Ratio

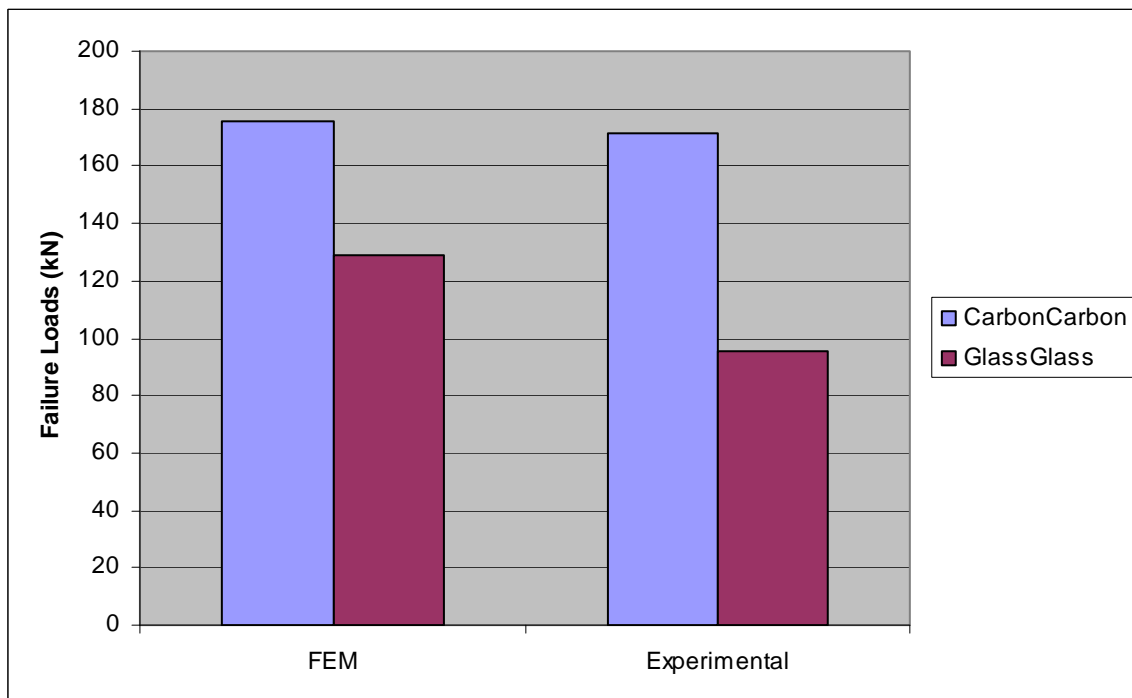


Figure 23. Failure Loads-8:1 Taper Ratio

C. SUMMARY

1. Angled Crack Model

Through the analysis, calculations and the application of different crack types and sizes, it was found that the model that best fit the experimental results was with an angle crack that took into account the taper ratio of the specimen. It was therefore decided to use this crack type throughout the rest of the analysis.

The classic VCCT and the Modified VCCT results were also compared in the previous section and it was found that the Modified VCCT gave better result and saved hours on each model while conducting the ANSYS analysis. The Interactive Biquadratic equation also produces better results, which are comparable to the experimental results obtained by NSWCCD.

THIS PAGE INTENTIONALLY LEFT BLANK

VI. FEM TENSILE AND COMPRESSIVE LOADS

Once the model has been validated, the materials were alternated between carbon and glass and forces applied.

A. TENSILE MODEL RESULTS

Carbon/carbon combination, as expected, shows the highest failure load under tension for both taper ratios, 4:1 and 8:1. There is a small variation between glass/carbon and carbon/glass; however, glass/carbon has a higher failure load as seen in Figure 24 and 25.

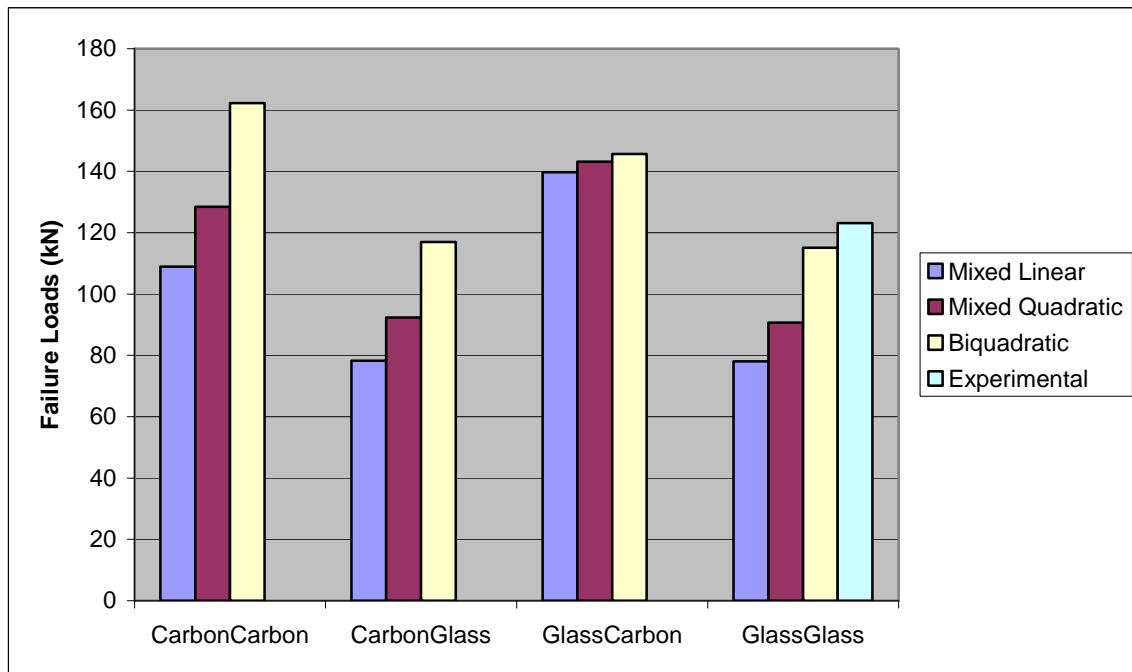


Figure 24. Load Prediction for 4:1 Taper Ratio Under Tension

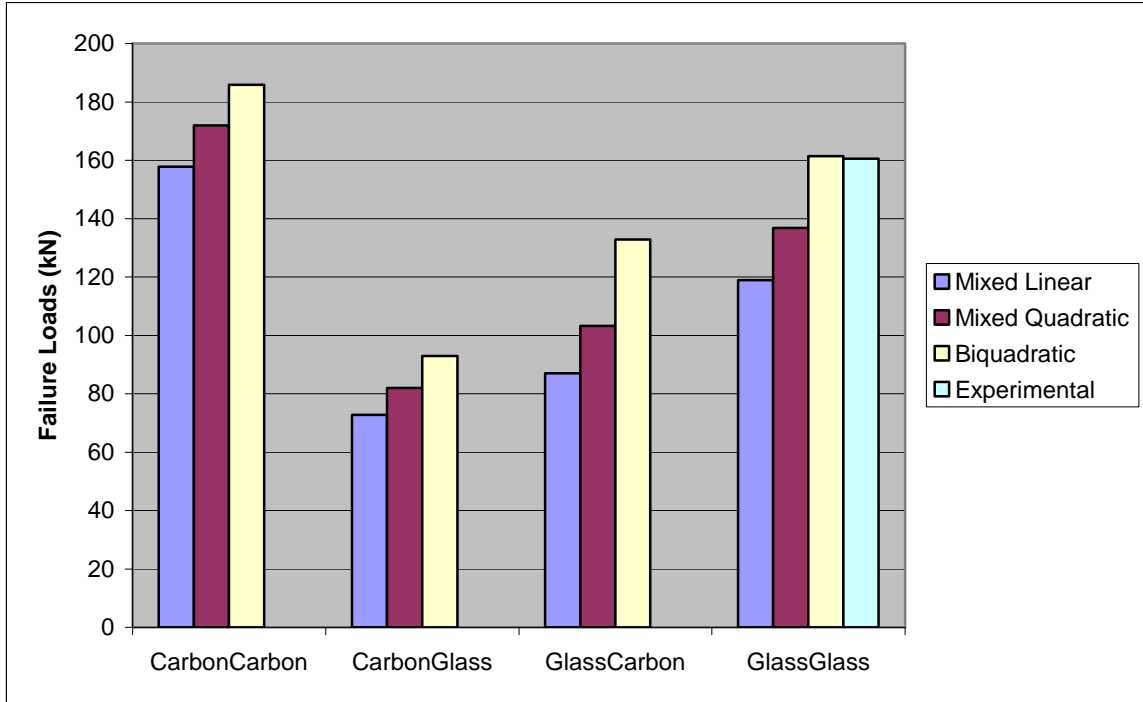


Figure 25. Load Prediction for 8:1 Taper Ratio Under Tension

B. COMPRESSION MODEL RESULTS

Using the same validated models as before, it was possible to calculate the stress in the scarf joint. From Figure 26 it can be seen that the highest stress is concentrated at the lower bottom tip of the joint.

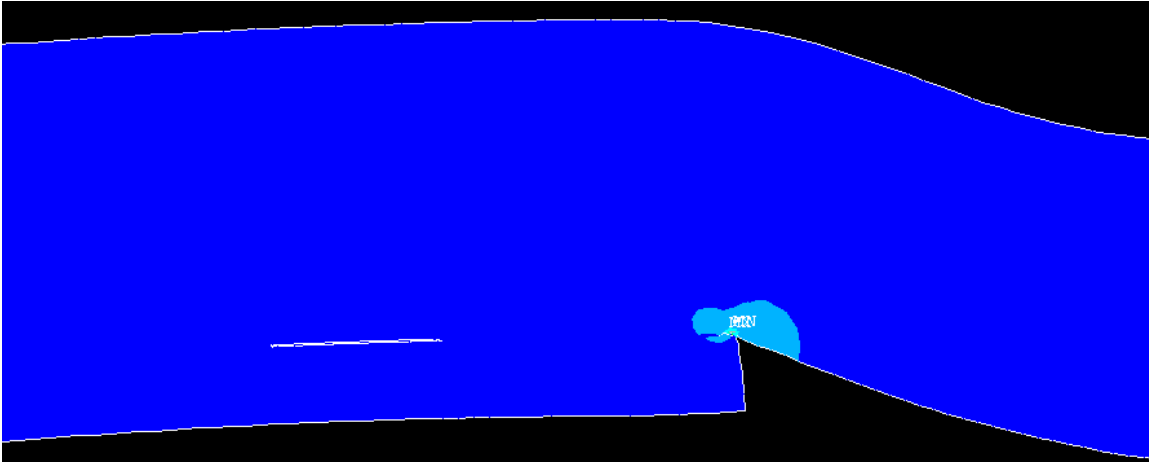


Figure 26. Scarf Joint in Compression

From the FEM analysis, both 4:1 and 8:1 taper ratio samples tended to bend up creating a clockwise moment at the crack tip as well as producing crack closure. Due to the crack closure and being small in size, it was extremely difficult to obtain an accurate reading of the forces and the nodal displacements at the crack tip. Therefore, the compression results are obtained by using the Interactive Biquadratic equation assuming G_f to be zero since there is crack closure.

The results for a taper ratio of 4:1 are shown in Figure 27 whereas the results for a taper ratio of 8:1 are on Figure 28.

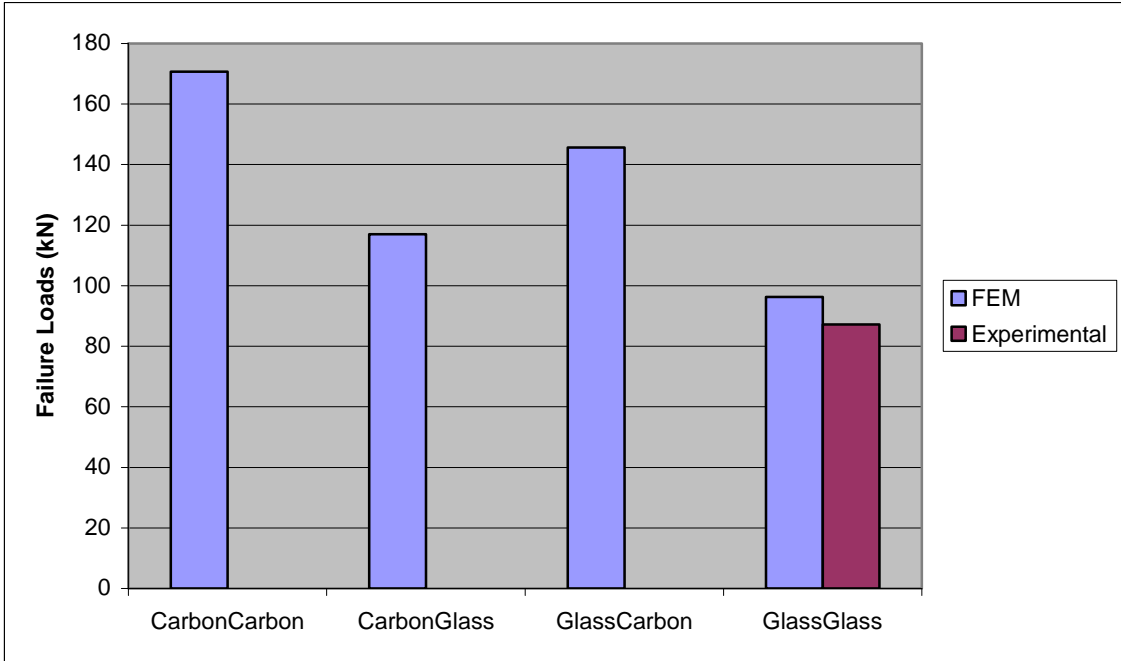


Figure 27. Scarf Joint in Compression-4:1 Taper Ratio

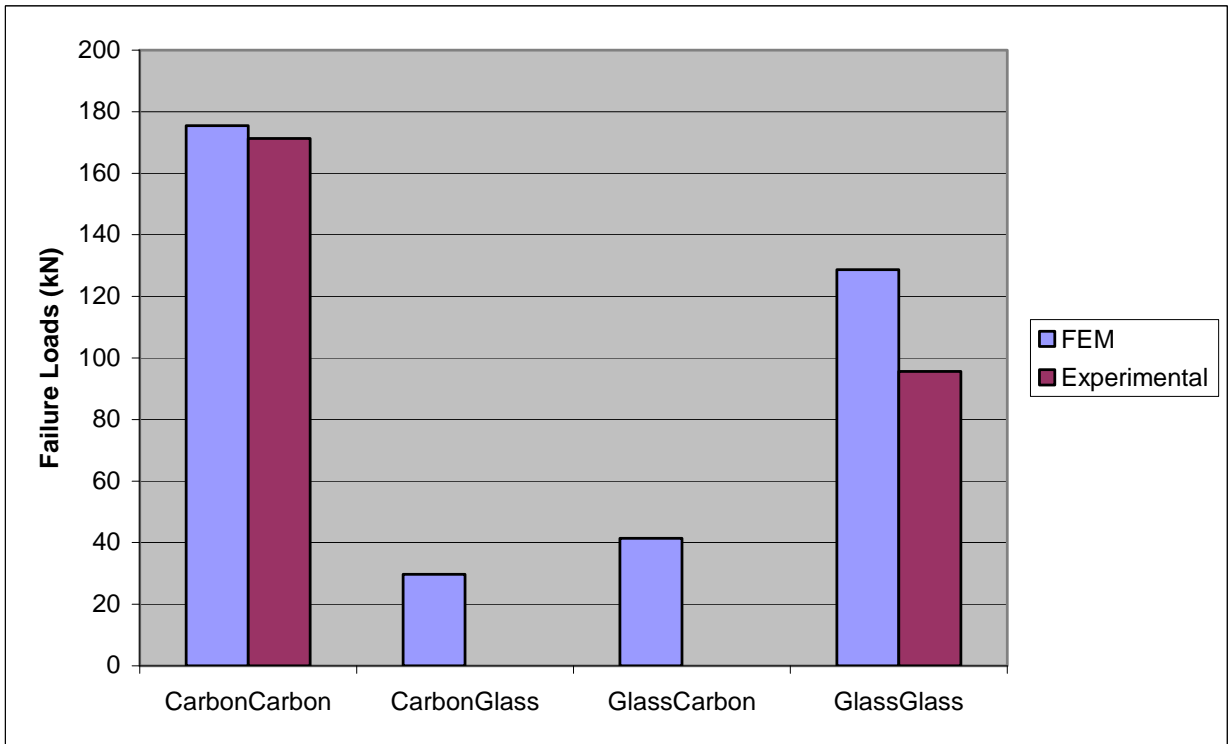


Figure 28. Scarf Joint in Compression-8:1 Taper Ratio

C. INFLUENCE OF CARBON AND GLASS COMBINATIONS

Due to the properties of the both carbon and glass fibers, the specimens reacted differently when forces were applied to the model. When the parent structure was made of carbon and the patch out of glass, the specimen rotates easily around the patch due to the flexibility of the material. In this case, most of the forces transfer more intensely to the critical point thereby decreasing its strength. On the other hand, when we have the parent structure made out of glass and the patch made out of carbon, the opposite occurs. In this case, the forces are distributed more evenly along the joint as the patch does not deform as readily and there is decreased moment at this critical point in the specimen.

What is interesting to note here is that the combination of glass and carbon produce a lower failure load than the glass/glass combination. This effect could be due to the disproportionate expansion or contraction of the two dissimilar materials causing greater strain at the joint.

THIS PAGE INTENTIONALLY LEFT BLANK

VII. ANALYSIS AND RESULTS FOR LOADING IN SHEAR

The section of highest stress is found through a simple analysis by applying a displacement of 0.02413cm in the $\pm y$ direction at the far right end while maintaining the left end fixed in all degrees of freedom. This displacement creates a counter clockwise moment. Figure 29 shows the stress concentrations on the model, which is produced by the moment created by the shear force. Although there are other areas of concentrated stress, particular attention is placed at the tip where the crack is more likely to initiate and propagate.



Figure 29. Model in Shear Showing Critical Locations

From the FEM model, it was observed that both opening and shearing forces, Mode I and II, are present in this region when the forces are applied in the $+y$ direction. This results in the most critical case.

A. ENERGY RELEASE RATE RESULTS

From Figures 30 and 31 it can be observed that the highest energy release, Mode II, is obtained for the carbon/carbon case. This is likely produced do to the

properties of carbon's high Young's modulus compared to that of glass or the resin, requiring a much greater force to displace the model by the same distance in the +y direction.

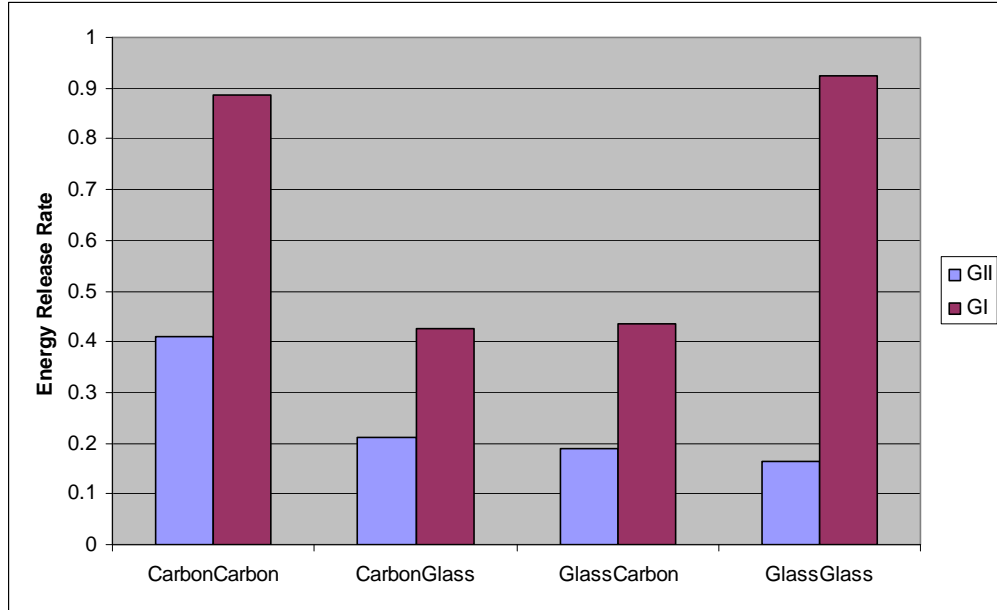


Figure 30. Energy Release Rate-4:1 Taper Ratio

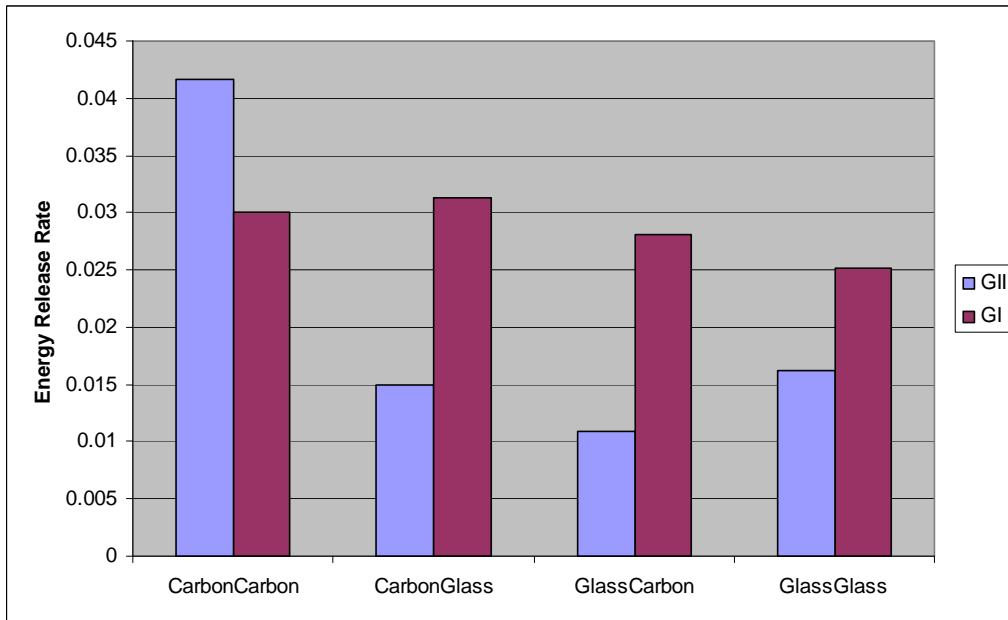


Figure 31. Energy Release Rate-8:1 Taper Ratio

B. SUMMARY

There does not seem to be a big difference in the energy release of the carbon/glass or glass/carbon combinations.

Maintaining the same model thickness, but with a taper ratio of 8:1, there is not much of a significant difference in the energy release rate compared to the 4:1, as shown in Figure 31, with the exception Mode I for carbon/carbon compared to that of the Figure 30.

THIS PAGE INTENTIONALLY LEFT BLANK

VIII. ANALYSIS AND RESULTS FOR LOADING IN BENDING

The shearing and opening of the crack under bending reacted very much like that of the shearing case resulting in Mode I and II.

A. ENERGY RELEASE RATE RESULTS

A CCW bending was considered as the most critical case since this produced both Mode I and II. Figures 32 and 33 show the comparison of the energy release between all four combinations.

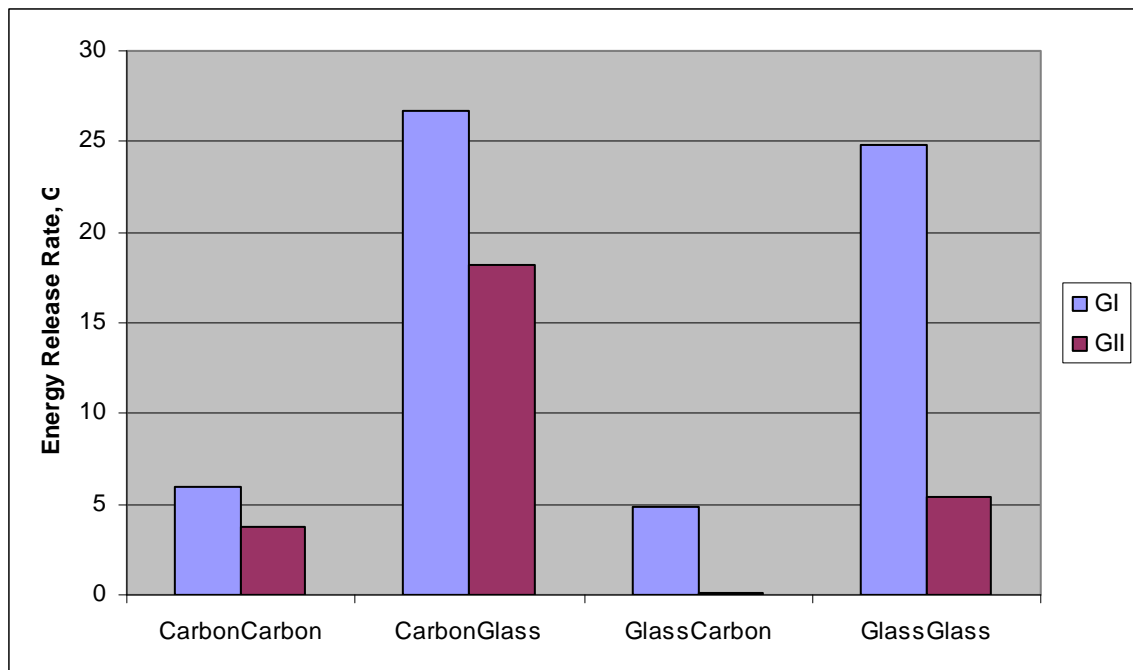


Figure 32. Energy Release Rate–In Bending (4:1 Taper Ratio)

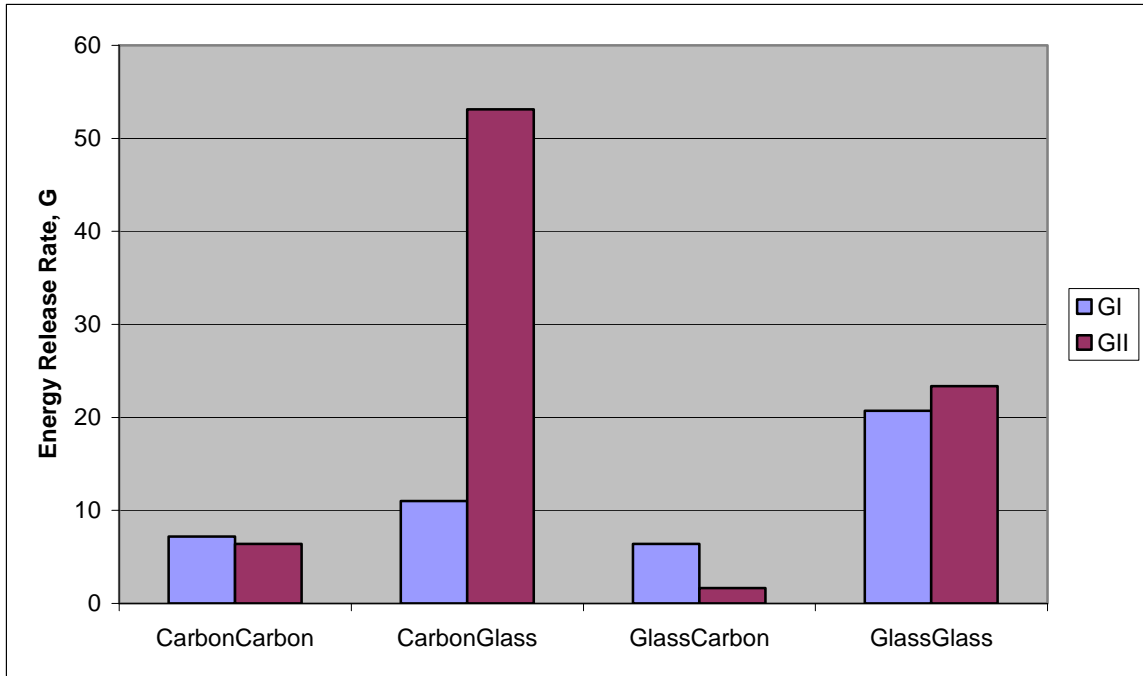


Figure 33. Energy Release Rate–In Bending (8:1 Taper Ratio)

B. SUMMARY

From the previous analysis, carbon/carbon and glass/carbon exhibit the lowest energy release rate compared to the other two combinations. In comparison, both 4:1 and 8:1 taper ratio, carbon/glass has greater energy release rates relative to the other two groupings.

IX. MODE II MODELING OF CARBON AND GLASS COMPOSITES

Models were created using ANSYS to model Mode II fracture on samples made of carbon and glass composites. These samples were tested in a three-point bending as shown in Figure 34.

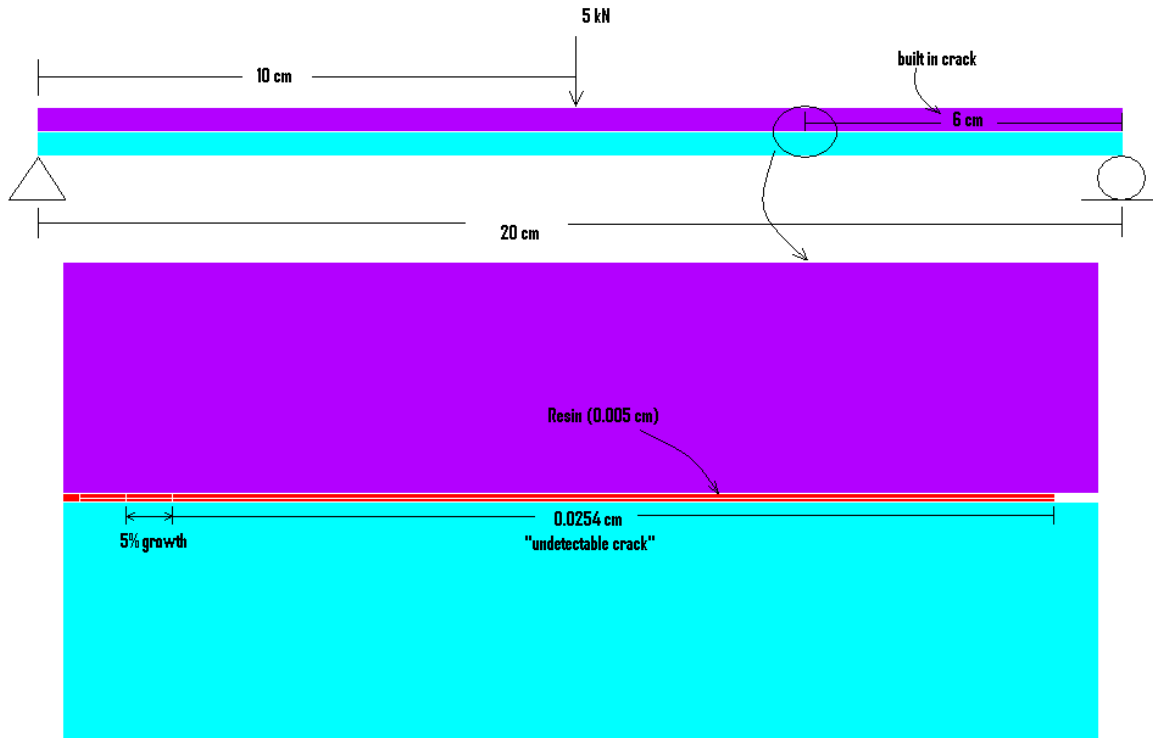


Figure 34. Three-point Bending Modeling

In this chapter, a glass/carbon combination means that the carbon is modeled on top while the glass is modeled on bottom as seen on the previous figure. These samples were created and alternated between carbon/carbon, carbon/glass, glass/carbon and glass/glass compositions. The samples were modeled with a resin interface of 0.005 cm in thickness and

extended from left side of the model up to the start of the built-in crack. The top and bottom composite slabs were of a 0.368 cm thickness.

When running the model, there was exceptional overlap between the top and bottom layers. This created a problem when trying to obtain the nodal forces and displacements. There are methods of avoiding this, such as the use of springs. For models previously described however, surface-to-surface contact elements were created using the built-in feature in ANSYS. This analysis gave a result with a minor overlap but did not interfere with obtaining the required displacement and force values.

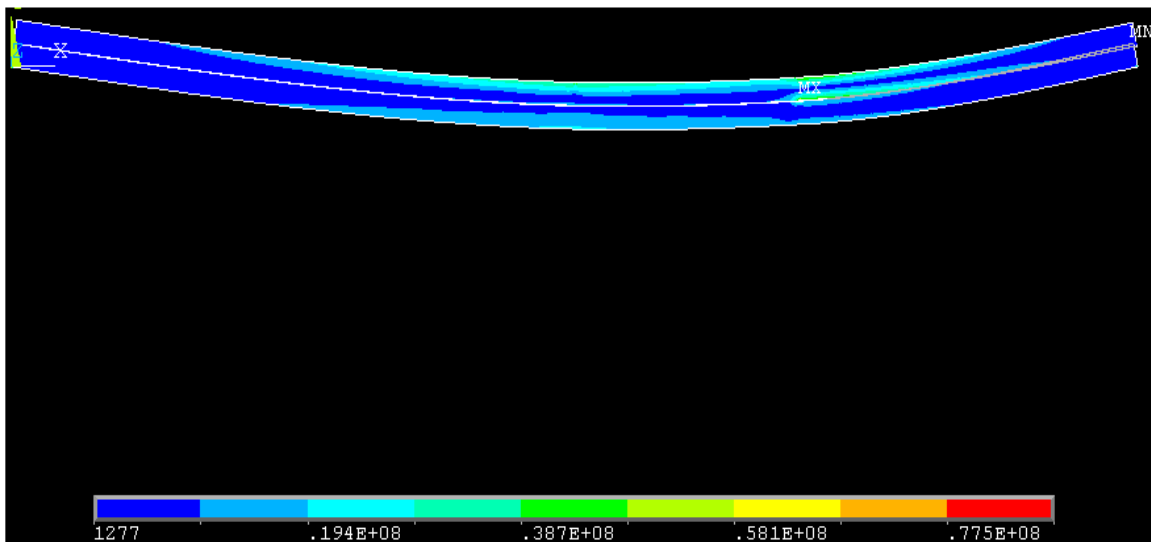


Figure 35. ANSYS Representation of Three-Point Bending von Mises Stress

From the analysis, there did not seem to be a big difference between the glass/carbon and carbon/glass combinations as shown from the energy release as shown in Figure 36 and Table 8.

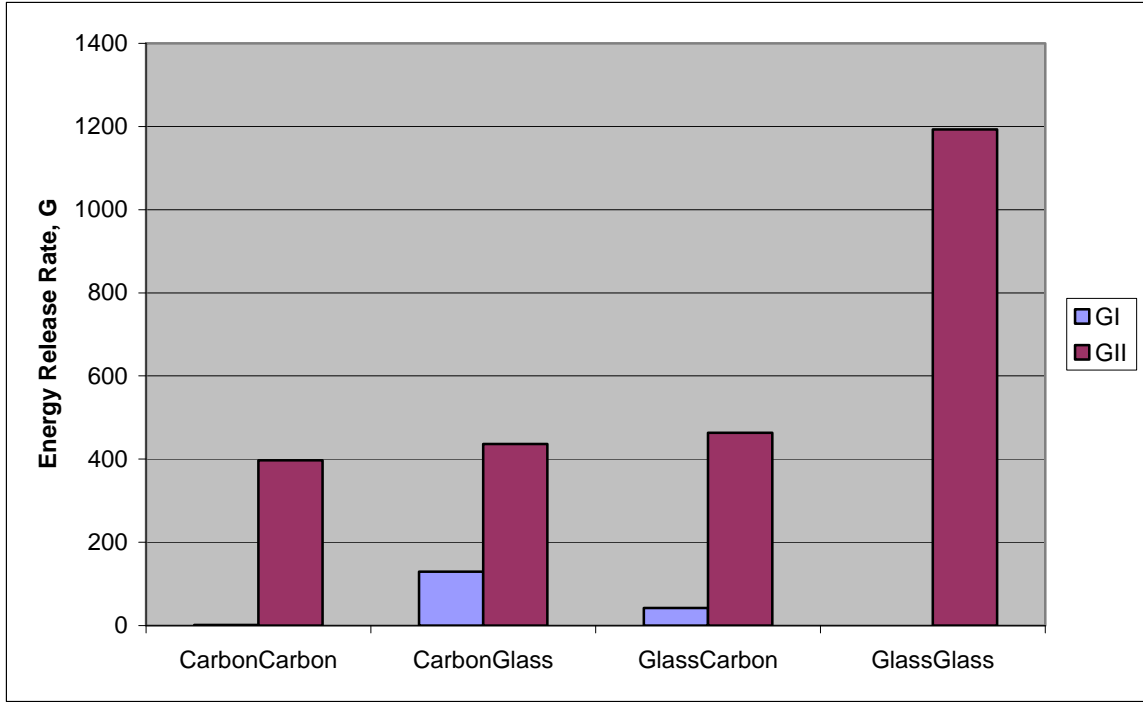


Figure 36. Energy Release Rate

Table 8. Fracture Toughness and Failure Load

	G_I	G_{II}	P_{fail}
Carbon/Carbon	0	397.3111	418.3938
Carbon/Glass	129.3878	436.0189	408.5042
Glass/Carbon	42.20438	463.1723	390.148
Glass/Glass	0	1193.098	241.375

The fracture toughness, G_I and G_{II} , was calculated using the Modified VCCT whereas the failure load was calculated using equation (5) with an 'm' value of -1.3. Using equations (3) thru(5), the following results are shown in Figure 37.

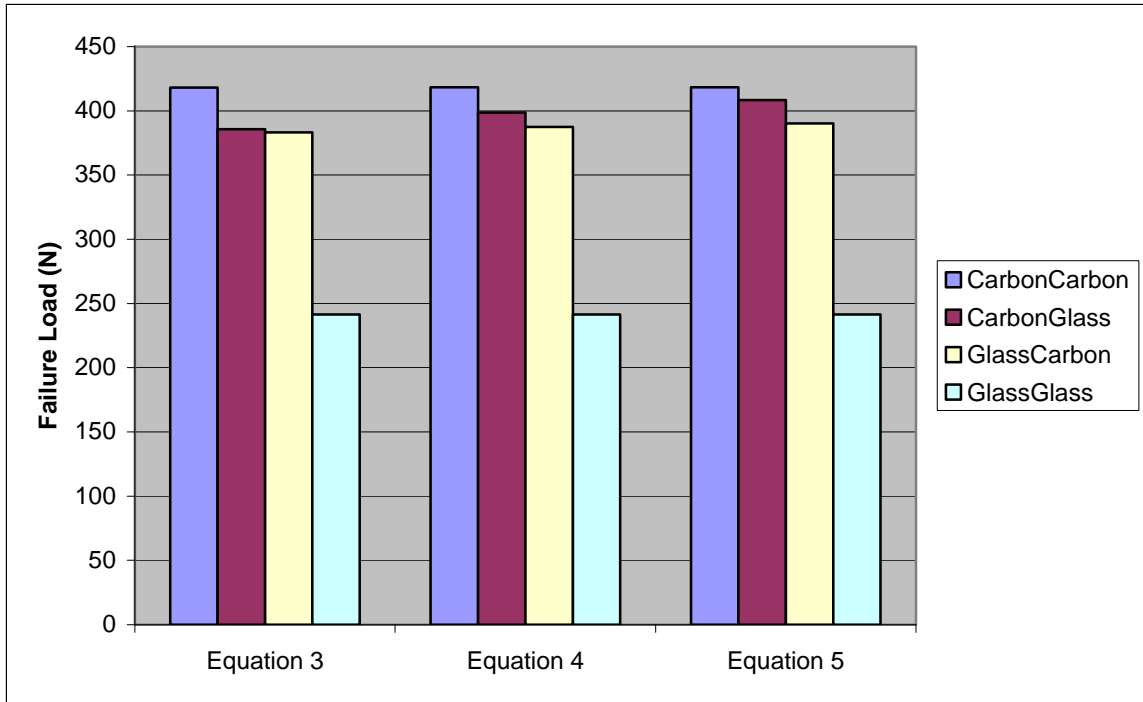


Figure 37. Failure Load Summary

From Figure 37 it is easy to see that the highest load resulted for a sample made of carbon/carbon and the lowest load was for a glass/glass composite.

X. CONCLUSIONS AND RECOMMENDATIONS

In the cases investigated in this study, proof was found that the carbon/carbon joint generally has greater strength than glass/glass. It is also found that the scarf joint between glass/carbon results in the lowest failure load. However, it might be unavoidable to have a joint made up of carbon and glass. It is this case that must be taken into careful consideration when making a joint, since this could be the weakest area.

The best modeling technique to predict failure was found by using a taper crack model, inserted in the resin interface that matched the taper ratio of the scarf joint, along with the modified virtual crack closure technique and the Interactive Biquadratic failure criterion. The MVCCT provided excellent results in a fraction of the time it would take to use the classic VCCT. Also, a constant value "m" of -1.3 gave accurate results that matched the experimental data using the Interactive Biquadratic failure equations. These results confirm the importance of the resin interface acting as an adhesive at the joint.

Specimens of carbon and glass combinations were constructed and tested to compare the scarf joint strength. From a group of 17 samples, seven failed through the joint under compression and the rest failed through the carbon interface as seen in Figures 8 and 9. These specimens were then modeled as isotropic with a resin layer interface with only Mode II, the Interactive Biquadratic failure criteria was used with G_I set to zero.

Through the experimental testing, it was observed that there could be countless small variations when creating the specimens, giving slightly different results. Several differences were noted in the models and samples compared to those of other reports. The process for creating the specimens resulted in samples that were almost 50% thinner than those created through the hand lay up. Although fewer layers of glass fibers were used to match the thickness of the carbon side, all failures happened in the carbon side or at the joint.

From the FEM model, a great deal of stress was generated at the joint due to the bending created by the applied forces. One way to balance the moment would be by creating a double scarf joint. Other types of joints, such as the stepped-lap joint, could also be studied for increased strength. This stepped-lap joint might cancel the moment created by the applied forces, thereby reducing the stress.

When joining two sections together at a shipyard could be relatively easy due to the controlled environment, however, out in the field one must be sure to know how all the variables that might affect the joints. These factors include humidity, surface preparation, scarf configuration, temperature and even the power of the vacuum used. It is difficult to determine delamination sources or geometric and material discontinuities as every sample is different. It is recommended to use specific joint configurations by standardizing the process involved in creating them, thereby reducing the uncertainty of the outcome.

LIST OF REFERENCES

- [1] R. Campilho, M. de Moura and J. Domingues, "Modeling Single and Double-Lap Repairs on Composite Materials," February 2005, Porto, Portugal.
- [2] R. Krueger, "The Virtual Crack Closure Technique: History, Approach and Applications," NASA/CR-211628, 2002.
- [3] T. Greene, "Analytical Modeling of Composite-to-Composite (SCARF) Joints in Tension and Compression," M.S. thesis, Naval Postgraduate School, Monterey, California, 2007.
- [4] R. Slaff, "The Enhancement of Composite Scarf Interface Strength Through Carbon Nanotube Reinforcement," M.S. thesis, Naval Postgraduate School, Monterey, California, 2007.
- [5] Orlet M. and Caiazzo, A. 1999. "Analysis Support of Integral Joint Parametric Testing," SAR-029-99, November 1999. Fort Washington, PA: Material Sciences Corporation.
- [6] D. P. Johnson, "Experimental examination of secondarily-bonded stepped lap joints under quasi-static and fatigue loading." Mississippi State University, MSUS. 3b, 2001.

THIS PAGE INTENTIONALLY LEFT BLANK

INITIAL DISTRIBUTION LIST

1. Defense Technical Information Center
Ft. Belvoir, Virginia
2. Dudley Knox Library
Naval Postgraduate School
Monterey, California
3. Professor Young W. Kwon
Naval Postgraduate School
Monterey, California
4. Douglas C. Loup
Naval Surface Warfare Center, Carderock Division
West Bethesda, Maryland
5. Engineering and Technology Circular Office, Code 34
Naval Postgraduate School
Monterey, California